

Response to Reviewer #2

We thank Reviewer #2 for their helpful comments and suggestions. The original comments are provided below in gray, and our responses, with specific revisions, noted in bold font.

Gunsch et al. present observations of aerosol concentration and composition at the University of Michigan Biological Station (UMBS) for July 2014. The authors use a combination of a high-resolution time-of-flight aerosol mass spectrometer, single particle aerosol time-of-flight mass spectrometer, and combination scanning mobility particle sizer spectrometer and aerodynamic particle size spectrometer to investigate the aerosol characteristics between 0.01 – 2.5 μm during this time period. The authors found four different air masses impacted the area during the time period: 2 air masses impacted by wildfires from Canada, 1 air mass impacted by cities south of UMBS, and 1 air mass from clean regions over Canada. The authors found an increase in particle number and mass, over the clean regime, for the air masses impacted by wildfires and cities; however, no matter where the air came from, it was always influenced by biomass burning. The paper provides important information about what influences the aerosol mass in a background, rural location, and is of value for Atmospheric Chemistry and Physics community; however, there are some concerns and some clarifications that need to be addressed first prior to publication.

Major Comments:

I'm wondering why the AMS data was not used more to help further validate the results from the single particle mass spectrometer, or to support some of the authors' hypotheses. For example, either PMF (Ulbrich et al., 2009), "poor-man's PMF" (Aiken et al., 2009; Zhang et al., 2005), or triangle plots of different fragments (Cubison et al., 2011; Hu et al., 2015; Ng et al., 2010) would further support the evidence of OA being strongly influenced by biomass burning, anthropogenic emissions, and biogenic emissions/chemistry (e.g., page 10, Lines 3 – 5 and page 11, lines 20 – 22). Without this support, speculations that biogenic emissions and chemistry leading to the very high O/C ratios observed is hard to interpret (page 11, lines 20 – 22). Other studies found high O/C ratios due to photochemical aging of the biomass burning emissions and aerosol (Liu et al., 2016; Zhou et al., 2017), which may have led to the high O/C instead of OA production from biogenic emissions. Also, cloud processing of the gases and OA may lead to high O/C ratios, along with the SO₄ (Sullivan et al., 2016). A discussion either including these various processes or a discussion that argues why one process over the others leads to the high O/C ratios is needed.

We added a time series plot of AMS m/z 60 and 73 (levoglucosan markers) to Figure S6, showing that biomass burning organic aerosol contributed to the OA measured and supporting the ATOFMS results in Figure 5. These data are now referred to on P12 L11-14 and P14 L3-5. On page 12, we now clarify the discussion and summarize that the observed elevated O/C ratio is likely due to both photochemical and aqueous-phase oxidation of both biogenic and biomass burning VOC precursors. Additional references were added as suggested. While we agree that extensive HR - AMS analysis would further support our findings, such analyses are unfortunately beyond the scope of what is feasible at this current time due to changes in personnel appointments following the field measurements. Given this limitation, we instead focus here in

detailed ATOFMS analyses and use the HR - AMS to support our findings, which we feel is a best compromise approach.

Throughout the Sections 3.2 – 3.4, in the comparisons of the different aerosol regimes, the aerosol number mode is mentioned. The biomass burning mode is the same as the background mode, and the urban mode is smaller than both the biomass burning and background mode; however, the authors discuss how chemistry and accumulation are occurring during transport of the biomass burning and urban air masses. A discussion about why the modes are similar (or smaller) while chemistry and accumulation is occurring is necessary for the readers to better relate these two possibly contradictory processes.

In order to explain the smaller urban air mass mode, P13 L19-22 now reads: “The particle mode of 69 ± 29 nm was also the smallest of the study (Figure S3) due to contributions from combustion emissions, typically less than 50 nm (Seinfeld and Pandis, 2016), which likely grew to the observed sizes due to the condensation of secondary species during transport. A similar mode of 84 ± 18 nm was observed by VanReken et al. (2015) at UMBS during summer 2009 urban air mass influence.” Based on the HYSPLIT backward air mass trajectories during urban air mass influence, the transport time from the nearest urban center was 24-36 h, which is less than the transport time from the Canadian wildfires (48 - 72 h), although it is difficult to compare expected particle growth during transport due to expected differences in precursor and oxidant species and concentrations.

To explain the similarities between the background and wildfire influence, P11 L10-12 now reads: “The particle number mode during wildfire influence was 80 ± 46 nm, similar to the background air mass period (mode of 82 ± 37 nm) (Figure S3).” As shown in Figure 3, the bulk submicron aerosol mass was similar between the background and wildfire influenced periods and dominated by oxygenated organics, showing that, while smoke influenced the site, the majority of the aerosol mass was secondary organic aerosol during both air mass influences. This is consistent with the significant transport time between the Canadian wildfires and the sampling location (48-72 h). While the ATOFMS identified the majority of >0.5 μ m particles as having biomass burning cores, the majority of the aerosol mass on these particles was secondary organic aerosol (P11 L24-27).

A more in - depth analysis of some of the aerosol characteristics would improve the results and the paper. For example, page 12, lines 6 – 11, the authors very briefly discuss an accumulation of SO₄ into the biomass burning particles; however, these particles are coming from wildfires in Canada. A discussion about where this SO₄ comes from would be beneficial, as recent studies have found a minor role for biomass burning emissions SO₄ and unclear for SO₂ emissions (Collier et al., 2016; Liu et al., 2016, 2017).

This is now addressed on P12 L 10-13: “SO₂ has been previously shown to be emitted from wildfires (e.g. Burling et al., 2010; Stockwell et al., 2014), and increases in particulate sulfate mass have been observed during wildfire plume aging through cloud processing (DeBell et al., 2004; Pratt et al., 2010).”

As another example, the authors found little NO₃ in the air masses impacted by urban regions (page 14, lines 7 – 10 and Figure 3) , which is surprising with the NO_x emissions and chemistry. What would have led to the extremely low amounts, especially since other downwind sites have observed enhanced NO₃ (Jimenez et al., 2009) ?

During urban influence, the AMS measured the highest concentrations of nitrate throughout the study (Figure 3). The present study is most comparable to the New England USA (urban downwind) and Pinnacle Park NY (remote) sites within Jimenez et al. (2009); these sites both have similar percentages of nitrate by mass compared to our study. These points are now stated on P14 L14-16.

Minor Comments

1) Page 1, line 27: “ The field site was also influenced . . . ” . It is not clear in the abstract what the influences are before this line.

We deleted “also”.

2) Page 2, line 21: Change leading primary particles to leading to primary particles

We made the suggested change.

3) Page 2, line 22: Why is water included as a secondary species for aerosol?

For most particles (with sea spray aerosol as a notable exception), water vapor partitions from the gas-phase to the particle phase, making water a secondary species.

4) Page 4, line 3: Any reason why Slowik et al. (2011) is not included in this comparison of SOA in Ontario?

This citation was added to P4 L4.

5) Page 5, line 19: Please check the Jimenez and DeCarlo, 2017 citation. The website listed for this citation leads to Canadian Interagency Forest Fire Centre.

This mistake was corrected.

6) Page 11, line 1: superscript the minus sign

This typo was corrected.

7) Page 11, line 12: Please change limit to limiting

This typo was corrected.

References

Burling, I., Yokelson, R.J., Griffith, D.W., Johnson, T.J., Veres, P., Roberts, J., Warneke, C., Urbanski, S., Reardon, J., Weise, D., 2010. Laboratory measurements of trace gas emissions from biomass burning of fuel types from the southeastern and southwestern United States. *Atmos. Chem. Phys.* 10, 11115-11130.

DeBell, L.J., Talbot, R.W., Dibb, J.E., Munger, J.W., Fischer, E.V., Frolking, S.E., 2004. A major regional air pollution event in the northeastern United States caused by extensive forest fires in Quebec, Canada. *J. Geophys. Res-Atmos.* 109, D19305.

Jimenez, J., Canagaratna, M., Donahue, N., Prevot, A., Zhang, Q., Kroll, J.H., DeCarlo, P.F., Allan, J.D., Coe, H., Ng, N., 2009. Evolution of organic aerosols in the atmosphere. *Science* 326, 1525-1529.

Liu, X., Zhang, Y., Huey, L., Yokelson, R., Wang, Y., Jimenez, J., Campuzano - Jost, P., Beyersdorf, A., Blake, D., Choi, Y., 2016. Agricultural fires in the southeastern US during SEAC4RS: Emissions of trace gases and particles and evolution of ozone, reactive nitrogen, and organic aerosol. *J. Geophys. Res-Atmos.* 121, 7383-7414.

Pratt, K.A., Heymsfield, A.J., Twohy, C.H., Murphy, S.M., DeMott, P.J., Hudson, J.G., Subramanian, R., Wang, Z., Seinfeld, J.H., Prather, K.A., 2010. In situ chemical characterization of aged biomass-burning aerosols impacting cold wave clouds. *J. Atmos. Sci.* 67, 2451-2468.

Seinfeld, J.H., Pandis, S.N., 2016. Atmospheric chemistry and physics: from air pollution to climate change. John Wiley & Sons, Hoboken, New Jersey.

Stockwell, C., Yokelson, R., Kreidenweis, S., Robinson, A., DeMott, P., Sullivan, R., Reardon, J., Ryan, K., Griffith, D., Stevens, L., 2014. Trace gas emissions from combustion of peat, crop residue, domestic biofuels, grasses, and other fuels: configuration and Fourier transform infrared (FTIR) component of the fourth Fire Lab at Missoula Experiment (FLAME-4). *Atmos. Chem. Phys.*, 9727.

Zhao, W., Hopke, P.K., Zhou, L., 2007. Spatial distribution of source locations for particulate nitrate and sulfate in the upper-midwestern United States. *Atmos. Environ.* 41, 1831-1847.

Zhou, S., Collier, S., Jaffe, D.A., Briggs, N.L., Hee, J., Sedlacek III, A.J., Kleinman, L., Onasch, T.B., Zhang, Q., 2017. Regional influence of wildfires on aerosol chemistry in the western US and insights into atmospheric aging of biomass burning organic aerosol. *Atmos. Chem. Phys.* 17, 2477-2493.

Ubiquitous Influence of Wildfire Emissions and Secondary Organic Aerosol on Summertime Atmospheric Aerosol in the Forested Great Lakes Region

Matthew J. Gunsch¹, Nathaniel W. May¹, Miao Wen², Courtney L. H. Bottenus^{2,3}, Daniel J. Gardner¹, Timothy M. VanReken^{2,†}, Steven B. Bertman⁴, Philip K. Hopke^{5,6}, Andrew P. Ault^{1,7}, Kerri A. Pratt^{1,8}

¹Department of Chemistry, University of Michigan, Ann Arbor, MI

²Department of Civil and Environmental Engineering, Washington State University, Pullman, WA

³Pacific Northwest National Laboratory, Richland, WA

⁴Department of Chemistry, Western Michigan University, Kalamazoo, MI

⁵Center for Air Resources, Engineering and Science, Clarkson University, Potsdam, NY

⁶Department of Public Health Sciences, University of Rochester School of Medicine and Dentistry, Rochester, NY

⁷Department of Environmental Health Sciences, University of Michigan, Ann Arbor, MI

⁸Department of Earth and Environmental Science, University of Michigan, Ann Arbor, MI

†Now at the National Science Foundation, Arlington, VA

Correspondence to: Kerri A. Pratt (prattka@umich.edu), Andrew P. Ault (aulta@umich.edu)

Abstract. Long-range aerosol transport affects locations hundreds of kilometers from the point of emission, leading to distant particle sources influencing rural environments that have few major local sources. Source apportionment was conducted using real-time aerosol chemistry measurements made in July 2014 at the forested University of Michigan Biological Station near Pellston, Michigan, a site representative of the remote forested Great Lakes region. Size-resolved chemical composition of individual 0.5 – 2.0 μm particles was measured using an aerosol time-of-flight mass spectrometer (ATOFMS), and non-refractory aerosol mass less than 1 μm (PM_1) was measured by a high resolution aerosol mass spectrometer (HR-AMS). The field site was ~~also~~ influenced by air masses transporting Canadian wildfire emissions and urban pollution from Milwaukee and Chicago. During wildfire influenced periods, 0.5 – 2.0 μm particles were primarily aged biomass burning particles (88% by number). These particles were heavily coated with secondary organic aerosol (SOA) formed during

transport, with organics (average O/C ratio of 0.8) contributing 89% of the PM₁ mass. During urban-influenced periods, organic carbon, elemental carbon/organic carbon, and aged biomass burning particles were identified, with inorganic secondary species (ammonium, sulfate, and nitrate) contributing 41% of the PM₁ mass, indicative of atmospheric processing. With current models under-predicting organic 5 carbon (OC) in this region and biomass burning being the largest combustion contributor to SOA by mass, these results highlight the importance for regional chemical transport models to accurately predict the impact of long-range transported particles on air quality in the upper Midwest United States, particularly considering increasing intensity and frequency of Canadian wildfires.

10 1 Introduction

Atmospheric particulate matter less than 2.5 μm in diameter (PM_{2.5}) has significant impacts on air quality, climate, and human health (Calvo et al., 2013; Pöschl and Shiraiwa, 2015). Atmospheric particles directly affect climate by scattering incoming solar radiation and indirectly by acting as cloud condensation (CCN) and ice nuclei (IN) (IPCC, 2013). Increased levels of PM_{2.5} are also linked to 15 increased health risks, particularly respiratory and cardiovascular diseases (Brook et al., 2004; Pope and Dockery, 2006). Particles can impact areas hundreds of kilometers from their sources through long-range transport, with residence times of up to two weeks depending on particle size and chemical composition (Uno et al., 2009). Determining the impact of the long-range transported particles, as well as how they are transformed in the atmosphere during transport, is a critical topic to accurately predict their air quality 20 and climate effects (Ault et al., 2011; Creamean et al., 2013). During transport, particles undergo heterogeneous reactions and gas-particle partitioning, aging the particles and leading to primary particles (e.g., soot) ~~to become becoming~~ internally mixed with secondary species, including water, ammonium, nitrate, sulfate, and oxidized organic carbon, thus changing the chemical composition of individual particles (Moffet and Prather, 2009; Riemer and West, 2013). These aging processes are particularly 25 important since chemical composition is directly related to particle properties, including reactivity, hygroscopicity, toxicity, scattering, and absorption properties (Brook et al., 2004; Pöschl, 2005; Calvo et al., 2013; Fierce et al., 2016). Particle properties also differ based on the distribution of chemical species, or mixing state, within a population of particles – whether various chemical species are contained within

a single particle (internally mixed) or within different particles (externally mixed). Particle mixing state representation in models is particularly important (Bauer et al., 2013), especially for predicting aerosol impacts on the climate (Matsui et al., 2013; Fierce et al., 2016).

Long-range transport of atmospheric particles can contribute to both remote and populated locations being out of compliance with air quality regulations (National Research Council and National Academies, 2010). For example, elevated aerosol mass and ozone in Europe, eastern Canada, and northeastern United States has been attributed to transported Canadian wildfire emissions (Forster et al., 2001; Colarco et al., 2004; Müller et al., 2005; Wang et al., 2010b; Dutkiewicz et al., 2011; Miller et al., 2011; Dempsey, 2013; Kang et al., 2014; Dreessen et al., 2016). A multi-day exceedance of the National Ambient Air Quality Standard for ozone in Maryland during the summer of 2015 was attributed to Canadian wildfire emissions (Dreessen et al., 2016). Similarly, elevated PM_{2.5} observed in New York and Wisconsin has been attributed to Ohio River Valley emissions. Transported pollutants can impact biogenic secondary organic aerosol (SOA) formation in remote locations (Carlton et al., 2010; Emanuelsson et al., 2013; Xu et al., 2015; Rattanavaraha et al., 2016). Finally, prior and on-going studies through the IMPROVE program in rural locations throughout North America have investigated both transported and local contributions to the aerosol populations (Hand et al., 2011). Uncertainty in the contributions of long-range aerosols and limited measurements in remote areas can lead to inaccuracies in modeling of aerosol source contributions.

Relatively few studies have chemically characterized atmospheric aerosols in the rural Great Lakes region of the United States (Sheesley et al., 2004; Kim et al., 2005; Kim et al., 2007; Zhang et al., 2009; Jeong et al., 2011; Sjostedt et al., 2011; Kundu and Stone, 2014; Bullard et al., 2017). Except for the major metropolitan areas of Detroit (MI), Chicago (IL), Minneapolis (MN), and Milwaukee (WI), much of the land is characterized by rural agricultural areas and remote forests without significant anthropogenic emissions. A study in the upper peninsula of Michigan conducted by Sheesley et al. (2004) observed major contributions from secondary organic aerosol from both biogenic and anthropogenic volatile organic compound (VOC) oxidation in the summer. Studies across rural Illinois and Ohio found major atmospheric contributions from secondary sulfate, nitrate, and organic carbon, consistent with aerosol aging during transport (Kim et al., 2005; Kim et al., 2007; Zhang et al., 2009), though these

locations were much less forested than the more northern Great Lakes regions. Kundu and Stone (2014) measured composition and sources at rural locations in Iowa, identifying major PM mass contributions from biomass burning, combustion, and dust. Jeong et al. (2011) and Sjostedt et al. (2011), and Slowik et al. (2011) identified contributions from secondary organic aerosol, elemental carbon, and dust in rural Harrow, Ontario, downwind of Detroit and Windsor. The scarcity of measurement data in the rural Great Lakes region provides limited opportunities for model evaluation and requires assumptions of background primary aerosol.

In remote regions, there are challenges in distinguishing and identifying primary and secondary aerosol sources, particularly for bulk methods (Pratt and Prather, 2012). Single-particle mass spectrometry allows the identification of particle sources through comparisons with source ‘fingerprints’ and particle aging through characterization of individual particle chemical mixing state (Pratt and Prather, 2009, 2012). Therefore, to apportion the sources of the aerosol population influencing northern Michigan, single particle mass spectrometry measurements were conducted during July 2014 at the University of Michigan Biological Station (UMBS) near Pellston, MI. In this study, individual particle chemical composition, measured in real-time using single-particle mass spectrometry, was used to identify the sources and secondary processing of transported particles at UMBS. In addition, high resolution aerosol mass spectrometry (HR-AMS) measured chemically-resolved mass concentrations of non-refractory aerosol (organics, sulfate, nitrate, ammonium, and chloride) to provide complementary mass-based characterization of the transported particles at UMBS.

20 2 Methods

2.1 Field Site and Instrumentation

Atmospheric measurements were conducted from July 13-24, 2014 at the University of Michigan Biological Station (UMBS) near Pellston, MI, a 10,000-acre, remote, forested location with little local pollution (Carroll et al., 2001). The closest major cities are Milwaukee (370 kilometers southwest), Detroit (385 kilometers south), and Chicago (466 kilometers southwest). Instrumentation was located

within a laboratory at the base of the Program for Research on Oxidants: Photochemistry, Emissions, and Transport (PROPHET) tower, a 30-meter tall sampling tower ($45^{\circ}33'31''\text{N}$, $84^{\circ}42'52''\text{W}$) (Carroll et al., 2001). Air was sampled from 34 m above ground level (\sim 14 m above the forest canopy) through foam-insulated 1.09-cm I.D. copper tubing at a flow rate of 9.25 L min^{-1} (laminar) with a residence time of 15 5 s. This tubing was connected to a shared sampling manifold at the base of the tower, allowing individual instruments to each have a dedicated sampling line while limiting particle loss.

An aerosol time-of-flight mass spectrometer (ATOFMS model 3800, TSI, Inc., Shoreview, MN) (Gard et al., 1997; Dall'Osto et al., 2004), described briefly below, was used to measure the size and chemical composition of individual atmospheric particles ranging from $0.5 - 2.0 \mu\text{m}$ in vacuum 10 aerodynamic diameter (d_{va}) (Section 2.2). An Aerodyne high resolution aerosol mass spectrometer (HR-AMS) (DeCarlo et al., 2006) measured chemically-resolved mass concentrations of non-refractory fine particulate material (nominal vacuum aerodynamic diameter range of $0.05 - 1.0 \mu\text{m}$) from July 15–24, 2014. Concentrations for major composition classes (organics, sulfate, nitrate, ammonium, and chloride) are reported here. O/C ratios were calculated throughout the study using the methods described by 15 Canagaratna et al. (2015). The operation of the HR-AMS followed standard practice as described elsewhere (Jayne et al., 2000; Allan et al., 2003; Jimenez et al., 2003; Allan et al., 2004); the sampling resolution for the UMBS observations was 2.5 min. Calibrations for instrument flow rate, particle sizing and transmission, and ionization efficiency were conducted during the study following documented 20 procedures (Jimenez and DeCarlo, 2017). Data were analyzed using SQUIRREL (version 1.60) and the high resolution analysis software tool PIKA (version 1.20) (Sueper, 2010), with the concentrations corrected based on the estimated composition-dependent collection efficiency (Middlebrook et al., 2012). Additional instrumentation included an ozone analyzer (Thermo Scientific model 49), a scanning mobility 25 particle sizer spectrometer (SMPS, TSI model 3936) with a sheath flow rate of 4 L/min and an aerosol flow rate of 0.4 L/min for measuring size-resolved number concentrations of mobility diameter particles 12-600 nm, and an aerodynamic particle sizer spectrometer (APS, TSI model 3321) for measuring size-resolved number concentrations of $0.5-19 \mu\text{m}$ aerodynamic diameter particles. SMPS and APS size distributions were merged to give a continuous aerosol distribution from $0.01-2.5 \mu\text{m}$ (aerodynamic

diameter) using previously established methods (Khlystov et al., 2004), assuming a density of 1.5 g cm^{-3} and shape factor of 1.

2.2 Aerosol Time-of-Flight Mass Spectrometer (ATOFMS)

Using the ATOFMS, 11,430 individual atmospheric particles ranging from $0.5 - 2.0 \mu\text{m}$ in d_{va} were chemically analyzed from July 13–24, 2014. The design and operation of the ATOFMS has been described in detail elsewhere (Dall'Osto et al., 2004; Su et al., 2004). Briefly, particles are focused through an aerodynamic lens system and optically detected by two 532 nm continuous wave lasers spaced 6 cm apart. Particle aerodynamic diameter is determined from particle velocity, which was calibrated using monodispersed spherical polystyrene latex spheres ($0.4 - 2.5 \mu\text{m}$, Polysciences, Inc.) of known diameter and density. Particles are individually desorbed and ionized by a 266 nm Nd:YAG laser that was operated at $\sim 1.2 \text{ mJ}$, and the resulting ions enter a dual-polarity reflectron time-of-flight mass spectrometer. Positive and negative ion mass spectra corresponding to the same individual particles are collected. Mass spectral peak lists for individual particles were generated using TSI MS-Analyze software.

The individual particle mass spectra were analyzed using YAADA (yaada.org), a software toolkit for MATLAB. Particles were clustered in YAADA using the ART-2a algorithm with a vigilance factor of 0.80 and a learning rate of 0.05 for 20 iterations (Song et al., 1999). The top 50 clusters were manually classified into five particle types described in section 3.1. These top 50 clusters contained 92% of the 11,430 particle mass spectra collected and are the focus of the manuscript. Particle identification was based on characteristic ATOFMS mass spectral signatures previously described (Silva et al., 1999; Pastor et al., 2003; Qin et al., 2012). The errors associated with number fractions for each particle type were calculated using binomial statistics.

To obtain chemically-resolved number and mass concentrations for $0.5-2.0 \mu\text{m}$ particles, ATOFMS particle counts were scaled with the APS size-resolved particle number concentration data using the method of Qin et al. (2006) to account for size-dependent particle transmission in the inlet. Briefly, ratios of APS number concentration to ATOFMS non-scaled number concentration were calculated every three hours for each individual size bin defined by the APS for use as a scaling factor.

This scaling factor was then multiplied by the corresponding ATOFMS number concentration, providing size and chemically-resolved particle number concentrations for each of the four particle types. These number concentrations were then converted to mass concentrations using assumed spherical shape and compositionally-specific densities. The following densities were applied for the four particle types: 1.5 g 5 cm^{-3} for biomass burning, 1.5 g cm^{-3} for salts, and 1.25 g cm^{-3} for organic carbon-sulfate (OC-sulfate) and elemental carbon/organic carbon – sulfate (ECOC-sulfate) particles (Spencer et al., 2007; Moffet et al., 2008).

3 Results and Discussion

3.1 Overview

10 The UMBS campaign (July 13-24, 2014) was characterized by air masses from three primary directions: north, northwest, and southwest (Figures S1 and S2), representative of periods observed during previous UMBS summer studies (Cooper et al., 2001; VanReken et al., 2015). Analysis of NOAA HYSPLIT backward air mass trajectories showed four distinct air mass time periods (Figure S2). From July 13–15, air primarily came from northwestern Canada. From July 15–17, the wind shifted and came from directly 15 north crossing over Lake Superior and Lake Michigan before arriving at the field site. In contrast, from July 17–22 the air came mainly from south-southwest of the field site, crossing over the major metropolitan areas of Chicago and Milwaukee followed by Lake Michigan. Finally, from July 23–24, air came from the north-northwest of the field site, crossing Lake Superior and Lake Michigan from northern Canada (Figure S2). During summer 2009, VanReken et al. (2015) found that 60% of the air masses came 20 from north/northwest of UMBS, similar to this study (57%). Air came from southern polluted regions 43% of the time during our study, compared to 29% during July-August 2009 (VanReken et al., 2015).

25 Total PM_{2.5} number, PM_{2.5} mass, and ozone concentrations ranged from 143 to 6,031 particles cm^{-3} (average \pm standard deviation: $1,822 \pm 1,181 \text{ particles cm}^{-3}$), 1 to 43 $\mu\text{g/m}^3$ (average \pm standard deviation: $8 \pm 8 \mu\text{g/m}^3$) and 9 to 63 ppb (average \pm standard deviation: $32 \pm 14 \text{ ppb}$), respectively (Figure 1). Maximum concentrations were detected when the air arrived from the southwestern urban areas, and

the minimum values were observed for air masses from the north during remote air transport (Figures S3 and S4). Previously, VanReken et al. (2015) observed an 85% increase in particle number concentration when air originating from these southwestern urban areas impacted UMBS. These results suggest a wide range of sources affecting the field site, which were directly observed by the ATOFMS. Here, we examine 5 the influences of wildfires (Section 3.3) and urban pollution (Section 3.4) on summertime aerosol chemical composition, compared to remote background (Section 3.2), at UMBS.

Major individual particle types observed by ATOFMS included biomass burning, organic carbon-sulfate (OC-sulfate), and elemental carbon/organic carbon-sulfate (ECOC-sulfate) (Figure 2). Biomass burning particles were characterized by intense peaks at m/z 39 (K^+) and -97 (HSO_4^-), as well as less 10 intense peaks at m/z 12 (C^+), 18 (NH_4^+), and 27 (C_2H_3^+) (Pratt et al., 2010). Biomass burning particles also contained a peak at m/z 43 ($\text{C}_2\text{H}_3\text{O}^+$), a marker for oxidized OC on particles, which is addressed further in section 3.3. Biomass burning was the most prominent particle type, comprising ~80% of 15 submicron (0.5 – 1.0 μm) and ~50% of supermicron (1 – 2 μm) particles, by number, throughout the study, with number fraction varying according to the level of influence from wildfires. OC-sulfate particles contributed ~7%, by number, to submicron (0.5 – 1.0 μm) particles and ~8%, by number, to 20 supermicron (1.0 – 2.0 μm) particles and were characterized by intense peaks at m/z 27 (C_2H_3^+), 39 ($\text{C}_3\text{H}_3^+/\text{K}^+$), +/-43 ($\text{C}_2\text{H}_3\text{O}^{+/-}$), and -97 (HSO_4^-). OC-sulfate particles can originate from a variety of sources including primary vehicular emissions (Toner et al., 2008) and secondary organic sources (Pratt and Prather, 2009). The intense m/z 43 (most intense OC-sulfate particle ion peak) is indicative of 25 significant SOA coatings on combustion particles, including biomass burning (Pratt and Prather, 2009). ECOC-sulfate particles, characterized by C_n^+ fragment peaks, observed at m/z 12 (C^+), 24 (C_2^+), 36 (C_3^+), 48 (C_4^+), etc., as well as markers at m/z 27 (C_2H_3^+), 18 (NH_4^+), and -97 (HSO_4^-), are attributed to vehicular emissions (Toner et al., 2006; Toner et al., 2008) and contributed ~5%, by number, to both sub- and supermicron particles with the majority observed on July 22 during an urban-influenced air mass. In addition to the previously mentioned combustion and secondary particles, Na and Ca salts internally mixed with nitrate were episodically detected, primarily during July 16–18 and July 24–25. Based on 25 elemental ratios and established mass spectral fingerprints,~~s~~ these salts ~~may have~~ originated from the Great Lakes (Axson et al., 2016)(Axson et al., 2016; May et al., 2018) and/or seawater, rather than mineral

dust (Sullivan et al., 2007; Ault et al., 2011; Fitzgerald et al., 2015), and are the focus of an upcoming manuscript. For each of the discussed particle types, we present the chemical mixing state by reporting the number percentage of particles within each particle type that contain a mass spectral marker corresponding to each secondary aerosol chemical species of interest, including sulfate (HSO_4^- , m/z -97),
5 nitrate (NO_2^- , m/z -46, and/or NO_3^- , m/z -62), ammonium (NH_4^+ , m/z 18), and oxidized OC ($\text{C}_3\text{H}_2\text{O}^-$, m/z -43, or $\text{C}_3\text{H}_2\text{O}^+$, m/z 43) (Qin et al., 2012).

PM₁ mass measured by the HR-AMS was on average 73% organics (7.8 $\mu\text{g}/\text{m}^3$) throughout the study, with a substantial contribution from oxidized organics as determined by an average HR-AMS O/C ratio of 0.84 and through the ATOFMS oxidized organic carbon ion marker m/z 43, $\text{C}_2\text{H}_3\text{O}^+$ (Aiken et al.,
10 2008; Qin et al., 2012). O/C ratios between 0.6 – 1 are commonly associated with low volatility oxidized organic aerosol (LV-OOA) that has undergone extensive aging (Jimenez et al., 2009), consistent with the single-particle observation that SOA coated the major particle types. In addition, the ammonium balance of predicted ammonium versus measured ammonium throughout the study (Figure S5) shows a slight deficit in measured ammonium, typically indicative of acidic aerosol or the presence of organic
15 nitrates/sulfates (Farmer et al., 2010). Also consistent with atmospheric processing during long-range transport, 92% of all 0.5 – 2.0 μm particles, by number, were measured by the ATOFMS to be internally mixed with secondary species, including sulfate (HSO_4^- , m/z -97), nitrate (NO_2^- , m/z -46 and/or NO_3^- , m/z -62), ammonium (NH_4^+ , m/z 18), and/or oxidized OC ($\text{C}_3\text{H}_2\text{O}^-$, m/z -43 or $\text{C}_3\text{H}_2\text{O}^+$, m/z 43) (Qin et al., 2012). On average, sulfate comprised 20% (2.2 $\mu\text{g}/\text{m}^3$) of the total PM₁ mass measured by HR-AMS.

20 3.2 Remote Background Air Mass Influence

From July 15-17, air arrived at UMBS originating from rural northern Canada. This remote background air mass period was differentiated from the wildfire influenced periods (Section 3.3) based on the lack of smoke impacting the site, as indicated by NOAA Smoke and Fire products (Figure 4). The average PM_{2.5} number concentration was 903 ± 499 particles cm^{-3} (range of 143 - 2163 particles cm^{-3} ,
25 Figure 1), and the average PM_{2.5} mass concentration was $1.9 \pm 0.4 \mu\text{g}/\text{m}^3$ with a particle number mode of 82 nm (Figure 1 and S3). comparable the average particle number ($1630 \pm 1280 \text{ cm}^{-3}$) and mode (73 ±

21 nm) observed by VanReken et al. (2015) during background air mass influence at UMBS in summer 2009. The average ozone concentration was 17 ± 6 ppb (Figure 1), similar to previous measurements at UMBS during background air mass influence (Cooper et al., 2001). Despite the ~~With a~~ lack of direct wildfire influence (Figure 4), $61 \pm 1\%$ of the $0.5 - 2.0 \mu\text{m}$ particles, by number, were classified by 5 ATOFMS as aged biomass burning aerosols, relatively similar to the background biomass burning particle influence reported by Hudson et al. (2004) and Pratt et al. (2010) for the United States free troposphere (33-52% by number). Biomass burning particles were internally mixed with oxidized OC (80 \pm 2%, by number) or mixed with sulfate (85 \pm 2%). Nitrate was internally mixed with 8 \pm 2%, by 10 number of biomass burning particles and 33 \pm 3%, by number, of OC-sulfate particles. It is likely that, while the observed biomass burning particles have a small potassium-rich (biomass burning) core, they are primarily SOA by mass (Pratt and Prather, 2009; Moffet et al., 2010) (Section 3.3). The HR-AMS showed average PM_1 organic mass concentrations of $4.4 \mu\text{g}/\text{m}^3$, with minimal contribution from sulfate (0.3 $\mu\text{g}/\text{m}^3$), as well as nitrate and ammonium (both less than $0.1 \mu\text{g}/\text{m}^3$ on average) (Figure 3).

The significant internal mixing of oxidized OC combined with the significant organic mass 15 loading (average HR-AMS O/C ratio of 0.9) is consistent with high SOA mass on the particles (Aiken et al., 2008). Previous studies in rural and forested environments found similarly high O/C ratios during periods of non-polluted air and attributed this to regional SOA formation (Jimenez et al., 2009; Sun et al., 2009; Raatikainen et al., 2010; Sjostedt et al., 2011). There was a notable spike in O/C ratio on July 15 – 16 to 1.2, indicative very highly oxidized organics. O/C ratios of this magnitude have previously been 20 observed at the remote Whistler Mountain, where organic aerosol O/C ratios up to ~ 1.3 were observed during organic aerosol accumulation events (Sun et al., 2009). Sheesley et al. (2004) found that SOA, primarily biogenic-derived, contributed over 90% of the total organic carbon mass observed during the summer at the Seney National Wildlife Refuge in northern Michigan, located 120 km northwest of UMBS. Notably, ultrafine particle growth was observed at UMBS on July 16 during this high O/C ratio 25 spike (Gunsch et al., 2017; Gunsch et al., 2018). The air arriving during this period was not under the influence of wildfires (Section 3.3) or urban areas (Section 3.4), and is therefore expected to be representative of remote background conditions.

3.3 Wildfire Influence

From July 13-15 and July 24 mid-day through July 25, the NOAA Hazard Mapping System (HMS) Smoke Product (Rolph et al., 2009) indicated that smoke plumes originating from wildfires within the Northwest Territories (Canada) directly influenced UMBS (Figure 4). According to the Canadian 5 Interagency Forest Fire Centre, over 5,500 km² of land burned within the Northwest Territories during July 2014 (CIFFC, 2014). Canadian wildfires are a major source of global PM_{2.5}, with estimates of ~1.6 Tg yr⁻¹ emitted to the atmosphere (Wiedinmyer et al., 2006). Average PM_{2.5} number and concentrations 10 during these two wildfire influence periods were statistically higher (t-test, $\alpha = 0.05$) at 1400 ± 800 particles cm⁻³ (range of 147 – 4832 particles cm⁻³, Figure 1) and $5.4 \pm 2.6 \mu\text{g}/\text{m}^3$ (range of 1.3 – 10.5 $\mu\text{g}/\text{m}^3$, Figure 1), respectively, compared to the background period (Section 3.2). The particle number 15 mode during wildfire influence was 80 ± 46 nm, similar to the background periods air mass period (mode of 82 ± 37 nm) (Figure S3). Ozone was also elevated during July 13-15 reaching as high as 35 ppb, compared to an average of 10 ppb during the background period (Figure 1). During these periods, the air masses did not pass over any major urban areas (Figure S2), making ozone production within the smoke 20 plume during transport the likely source (Jaffe and Wigder, 2012). Ozone did not increase during the July 24 smoke plume, staying near the average for the study (25 ± 12 ppb) with a concentration of 26 ± 3 ppb (Figure 1). While an ozone increase is often observed for aged wildfire plumes, an increase does not always occur during wildfire influence, such as when low NO_x levels within plumes, potentially due to smoldering combustion, limiting the production of ozone (Jaffe and Wigder, 2012).

Formatted: Superscript

Formatted: Font: Bold

During the wildfire influenced periods, $88 \pm 1\%$ of the measured 0.5 – 2.0 μm particles, by 25 number, were biomass burning particles, with an average mass concentration of $0.42 \mu\text{g}/\text{m}^3$ (Figure 5) and a maximum of $0.80 \mu\text{g}/\text{m}^3$ occurring during the early afternoon of July 14 when the heaviest wildfire smoke was reported by the NOAA smoke product (Figure 4A). Minor contributions of OC-sulfate particles ($8 \pm 1\%$ by number) were also measured. The OC-sulfate particle mass spectra (Figure 2B) showed that $75 \pm 5\%$, by number, contained potassium (K^+ , m/z 39), suggesting that these were highly aged biomass burning particles coated by SOA such that the typical biomass burning mass spectral signature had been masked, as observed previously by Pratt and Prather (2009) using a thermodenuder.

These OC-sulfate particles featured a dominant intense m/z 43 ($\text{C}_2\text{H}_3\text{O}^+$) ion peak, indicating that these particles were heavily coated with SOA. During the afternoon event on July 24, PM_1 organic mass concentrations measured by HR-AMS nearly doubled from $2.5 \pm 0.1 \mu\text{g}/\text{m}^3$ before the event to $4.5 \pm 0.3 \mu\text{g}/\text{m}^3$ during the event (Figure 3), accounting for ~90% of the total PM_1 mass concentration. The HR-
5 AMS O/C ratio was 0.8 during wildfire periods, consistent with biomass burning particles heavily coated with SOA (Aiken et al., 2008), as also observed by $95 \pm 1\%$, by number, of the biomass burning and OC-sulfate particles, measured by ATOFMS during these periods, featuring the oxidized OC ion marker (m/z 43, $\text{C}_2\text{H}_3\text{O}^+$) (Figure 6). Freshly emitted biomass burning has a O/C ratio of ~0.2, which can increase to ~0.6 in only a few hours as the emissions undergo photochemical aging and oxidized material condenses
10 onto the particles (Grieshop et al., 2009; Pratt et al., 2011)(Grieshop et al., 2009; Pratt et al., 2011; Liu et al., 2016; Zhou et al., 2017). While AMS levoglucosan ion markers (m/z 60 ($\text{C}_2\text{H}_4\text{O}_2^+$) and 73 ($\text{C}_3\text{H}_5\text{O}_2^+$))
15 (Alfarra et al., 2007) were observed, consistent with the ATOFMS observation of biomass burning particles, the levels were low (Figure S6), due to the expected degradation during atmospheric transport (Hennigan et al., 2010). As +T_{he} wildfire air masses measured during the present study were transported
18 48 – 72 h over multiple days over Canadian forests, suggesting the accumulation of both biomass burning SOA and biogenic SOA, from condensation of monoterpene oxidation products (Slowik et al., 2010), likely contributed to the observed O/C ratio of 0.8 at UMBS. Previous studies conducted by Slowik et al. (2010) and Sheesley et al. (2004) observed monoterpene-derived SOA within summertime air masses passing over these forest. Therefore, it is likely that the oxidation (both gas- and aqueous-phase) of both
20 biomass burning and biogenic VOCs (Lee et al., 2011), contributed to the observed elevated O/C ratio of 0.8 - 1.1 at UMBS.

During transport of the biomass burning aerosols, accumulation of sulfate also occurred, with $97 \pm 1\%$, by number, of biomass burning particles internally mixed with sulfate (m/z -97, HSO_4^-) (Figure 6). HR-AMS measured PM_1 sulfate also increased from less than $0.1 \mu\text{g}/\text{m}^3$ to $2 \mu\text{g}/\text{m}^3$ after mid-day July 24 (Figure 3). Increases SO_2 has been previously shown to be emitted from wildfires (e.g. Burling et al., 2010; Stockwell et al., 2014), and increases in particulate sulfate mass have been observed during wildfire plume aging through cloud processing (DeBell et al., 2004; Pratt et al., 2010). In comparison, the HR-
25

AMS measured limited amounts of PM_1 ammonium (~2% of total mass, $0.2 \mu\text{g}/\text{m}^3$) during the wildfire event on July 24 (Figure 3). However, ammonium was internally mixed in $38 \pm 2\%$, by number, of biomass burning and $68 \pm 2\%$, by number, of OC-sulfate particles (Figure 6). This result indicates that while ammonium was present within many particles, it was a minor fraction of the particle mass. Nitrate 5 was also internally mixed with $43 \pm 2\%$ of biomass burning particles, by number, and $17 \pm 2\%$, by number, of OC-sulfate particles (Figure 6), and the HR-AMS only measured ~1% of PM_1 mass to be nitrate ($0.06 \mu\text{g}/\text{m}^3$). Therefore, it is likely that the ammonium was present in the form of ammonium sulfate internally mixed with biomass burning and OC-sulfate.

3.4 Urban Air Mass Influence

10 From July 17-22, UMBS was influenced by air masses from the southwest, passing over the major metropolitan areas of Chicago and Milwaukee before arriving at the site (Figure S2) after transport times of 24-36 hours. Stagnant air (wind speeds of ~ 2 m/s) led to the buildup of the urban-influenced PM, which peaked on July 22, as shown in Figure 1. The passing of a cold front, along with precipitation and a change in wind direction, led to a sudden decrease in PM concentration late on July 22 (Figure 1). The 15 average ozone concentration was elevated at an average of $41 \pm 12 \text{ ppb}$ similar to previous measurements by Cooper et al. (2001) at UMBS when under the direct influence of urban pollution (Figure 1). The $\text{PM}_{2.5}$ number and mass concentration for this period were $2,700 \pm 900 \text{ particles cm}^{-3}$ (range of $414 - 6,031 \text{ particles cm}^{-3}$) and $14 \pm 8 \mu\text{g}/\text{m}^3$ (range of $2 - 43 \mu\text{g}/\text{m}^3$), respectively, the highest for the study (Figure 1). The particle mode of $69 \pm 29 \text{ nm}$ was also the smallest of the study (Figure S3) due to contributions from combustion emissions, typically less than 50 nm (Seinfeld and Pandis, 2016), which likely grew to the observed sizes due to the condensation of secondary species during transport. A similar mode of $84 \pm 18 \text{ nm}$ was observed by VanReken et al. (2015) at UMBS during summer 2009 urban air mass influence. 20 VanReken et al. (2015) also previously observed the highest particle number concentrations ($3,000 \pm 1,300 \text{ particles cm}^{-3}$) at UMBS during the influence of southern air masses. Wildfire smoke~~Smoke~~ influence was present during this period as shown by the NOAA smoke product (Figure 4C). However, 25 unlike during the previous periods, this smoke originated mainly from the southern United States ~~(active~~

fires were located in Tennessee, Arkansas, and Missouri), and were from agricultural and forest fires (active agricultural fires were located in Missouri, with a forest fire in Arkansas). The HR-AMS showed levoglucosan ion markers (m/z 60 ($C_2H_4O_2^+$) and 73 ($C_3H_5O_2^+$)) (Alfarra et al., 2007) (Figure S6), consistent with the satellite-observed smoke influence.

Biomass burning particles measured by ATOFMS

5 steadily increased in mass concentration throughout this period (Figure 5), with a notable spike in the mass concentration on July 22 observed in both the submicron (0.5-1.0 μm particles: 2.3 $\mu g/m^3$) and supermicron (0.3 $\mu g/m^3$) size ranges (1.0-2.0 μm particles: Figure 5). Overall, during urban influence, biomass burning particles accounted for 72 \pm 2% of the particles, by number, and \sim 30% of the total mass concentration (Figure 5). The biomass burning particles were aged, as shown by internal mixtures of

10 sulfate (88 \pm 2%, by number), oxidized OC (92 \pm 1%, by number), ammonium (58 \pm 2%, by number), and nitrate (30 \pm 2%, by number) (Figure 6). The greatest internal mixing with ammonium was observed during this period. Notably, a higher number fraction of the biomass burning particles during this period were internally mixed with ammonium, compared to the biomass burning particles detected during the Canadian wildfire influence.

15 The HR-AMS also measured the highest average ammonium mass concentration during this period of 1.6 $\mu g/m^3$, accounting for 10% of the total PM_1 particle mass (Figure 3). Agricultural activities, both crop and livestock, located to the south and southwest of the field site (Stephen and Aneja, 2008; Paulot et al., 2014) may be the source of the elevated ammonium levels.

ECOC-sulfate and OC-sulfate particles comprised the second most prominent particle types measured by ATOFMS during this urban-influenced period at 12 \pm 1% and 9 \pm 1% of the submicron (0.5 – 1.0 μm) particles, by number, and an average of 0.08 $\mu g/m^3$ and 0.03 $\mu g/m^3$, respectively (Figure 5). The influence of urban vehicular combustion resulted in the increased levels of measured ECOC-sulfate particles (Toner et al., 2006; Toner et al., 2008), compared to non-urban influenced periods (2 \pm 1% by number). HR-AMS PM_1 mass concentrations (Figure 3) showed increased organic mass during urban influence with an average mass concentration of 9.7 $\mu g/m^3$ (Figure 3), likely due to a mixture of biomass burning, anthropogenic, and biogenic organic aerosol. The average HR-AMS O/C ratio during the urban period was the lowest of the study (0.78), likely due to increased contributions from hydrocarbon-like organic aerosol from urban vehicle combustion emissions (Aiken et al., 2008), in contrast to primarily

oxidized organic aerosol during regional background periods (Jimenez et al., 2009). An increase in less oxidized organic aerosol was similarly observed in rural Ontario when the site was influenced by urban air masses from Detroit, compared to remote air masses (Sjostedt et al., 2011). The ECOC-sulfate and OC-sulfate particles were highly aged, with ~75%, by number, of each particle type internally mixed with 5 ammonium, consistent with particle aging during transport (Figure 6C). Ammonium (1.6 $\mu\text{g}/\text{m}^3$) and sulfate (4.9 $\mu\text{g}/\text{m}^3$) comprised over 40% of the total PM_1 mass measured by the HR-AMS during these periods, likely in the form of ammonium sulfate (Figure 3). Urban influenced air masses had the highest mass concentration of sulfate (up to 10 $\mu\text{g}/\text{m}^3$) measured throughout the study. In contrast, there was little presence of nitrate internally mixed in the ECOC-sulfate (4 \pm 2%, by number) and OC-sulfate (19 \pm 5%, 10 by number) particles (Figure 6). Finally, while, and nitrate only comprised 1% (0.2 $\mu\text{g}/\text{m}^3$) of the total PM_1 mass concentration during from the urban influence (Figure 3). , this was the highest nitrate contribution during the study, similar previous rural eastern United States studies (Jimenez et al., 2009).

4 Conclusions

Source apportionment of atmospheric particles in the summertime was conducted at the forested 15 University of Michigan Biological Station, located in remote northern Michigan. The field site was impacted by air masses from three distinct areas: remote background, northwestern Canada, and southwestern urban areas. July 2014 was one of the most active burning seasons for the Northwest Territories in over two decades with a total of 10,643 km^2 of land burned, significantly more than the ten-year (1,944 km^2) and twenty-five year (2,423 km^2) averages (CIFFC, 2014). The increased wildfire 20 activity noticeably impacted northern Michigan, as the presence of biomass burning particles was ubiquitous throughout the study and made up the majority of measured particle number and mass concentrations. While air also came from urban areas southwest of UMBS, aged biomass burning particles dominated particle number concentrations due to wildfire influences from the southern United States. Due to the urban influence, these air masses had the highest mass contributions of sulfate (over 50 times 25 the background) detected during the entire study. The accumulation of soluble secondary species,

including sulfate and nitrate, increases the CCN ability of biomass burning particles (Furutani et al., 2008; Petters et al., 2009; Wang et al., 2010a), illustrating the importance of transported wildfire emissions.

While biomass burning particles were the most dominant particle core detected, SOA was a major contributor to particle mass during the study. On average, the HR-AMS organic aerosol O/C ratio was 0.84, indicative of highly oxidized organic carbon (Aiken et al., 2008). During remote background periods, internal mixing of oxidized OC combined with the significant PM₁ organic mass loading is indicative of the high mass loading of biogenic SOA in the forested region (Sheesley et al., 2004). During wildfire-influenced air masses, organics contributed ~90% to the PM₁ mass, with SOA internally mixed with biomass burning and OC-sulfate particles, indicating that SOA from both biogenic VOC oxidation and wildfire combustion is a major source of OC in the region. The observed levels of biomass burning aerosol influence are attributed to the abnormally active Canadian wildfire season of 2014, compared to previous typical summers in northern Michigan with primarily biogenic SOA influence (Sheesley et al., 2004). Models under-predict OC in this region, and Jathar et al. (2014) indicates that on a national level, models predict biomass burning is the largest combustion contributor to SOA by mass, consistent with the significant influence of wildfires during this work.

Modeling studies have called for further investigations of wildfire emissions and areas they affect in order to reduce uncertainty within models due to limited data, particularly when modeling interactions between wildfire plumes and urban emissions. Wildfire plume ozone production can lead to areas far from the original source to be out of compliance with regulatory standards, demonstrating the importance to be able to accurately model ozone production (Hu et al., 2008; Jaffe and Wigder, 2012; Lu et al., 2016). Also, as described here, particles aged through transport show internal mixtures of nitrate, sulfate and oxidized organics, which can lead to increased CCN activity (Furutani et al., 2008). With wildfires expected to increase in both intensity and frequency due to climate change (Gillett et al., 2004; Liu et al., 2010; Knorr et al., 2016; Veira et al., 2016), the contributions of long-range transported biomass burning emissions to the upper Midwest US atmosphere are expected to increase, such that air quality modeling efforts will need to supplement their existing emissions to account for the expected increase in wildfire emissions (Smith and Mueller, 2010).

Competing Interests. The authors declare that they have no competing financial interests.

Acknowledgements. Funding for the UMBS study was provided by University of Michigan MCubed Program and UMBS graduate fellowships for M. Gunsch, N. May, and D. Gardner. We also thank the Pratt and Ault Groups for assistance on the field study. Support for T. VanReken and M. Wen was

5 provided by the U.S. Department of Energy Early Career Research Program (award no. SC0003899).

Jennifer Dean (Washington State University) is thanked for her assistance during the field study. Donna Sueper (Aerodyne) is thanked for assistance with HR-AMS data processing. The authors gratefully acknowledge the NOAA Air Resources Laboratory (ARL) for the provision of the HYSPLIT transport and dispersion model and READY website (<http://www.ready.noaa.gov>) used in this publication. The

10 authors also gratefully acknowledge the NOAA Office of Satellite and Product Operations for the use of the Hazard Mapping System Smoke Product (<http://www.ospo.noaa.gov/Products/land/hms.html>).

References

Aiken, A. C., Decarlo, P. F., Kroll, J. H., Worsnop, D. R., Huffman, J. A., Docherty, K. S., Ulbrich, I. M., Mohr, C., Kimmel, J. R., and Sueper, D.: O/C and OM/OC ratios of primary, secondary, and ambient organic aerosols with high-resolution time-of-flight aerosol mass spectrometry, Environ. Sci. Technol., 42, 4478-4485, 2008.

5 [Alfarra, M. R., Prevot, A. S., Szidat, S., Sandradewi, J., Weimer, S., Lanz, V. A., Schreiber, D., Mohr, M., and Baltensperger, U.: Identification of the mass spectral signature of organic aerosols from wood burning emissions. Environ. Sci. Technol., 41, 5770-5777, 2007.](#)

Allan, J. D., Jimenez, J. L., Williams, P. I., Alfarra, M. R., Bower, K. N., Jayne, J. T., Coe, H., and Worsnop, D. R.: Quantitative sampling using an Aerodyne aerosol mass spectrometer 1. Techniques of data interpretation and error analysis, J. Geophys. Res-Atmos., 108, 4090, 2003.

10 Allan, J. D., Delia, A. E., Coe, H., Bower, K. N., Alfarra, M. R., Jimenez, J. L., Middlebrook, A. M., Drewnick, F., Onasch, T. B., and Canagaratna, M. R.: A generalised method for the extraction of chemically resolved mass spectra from Aerodyne aerosol mass spectrometer data, J. Aerosol. Sci., 35, 909-922, 2004.

15 Ault, A. P., Williams, C. R., White, A. B., Neiman, P. J., Creamean, J. M., Gaston, C. J., Ralph, F. M., and Prather, K. A.: Detection of Asian dust in California orographic precipitation, J. Geophys. Res-Atmos., 116, 2011.

20 Axson, J. L., May, N. W., Colón-Bernal, I. D., Pratt, K. A., and Ault, A. P.: Lake Spray Aerosol: A Chemical Signature from Individual Ambient Particles, Environ. Sci. Technol., 50, 9835 - 9845, 2016.

Bauer, S. E., Ault, A., and Prather, K. A.: Evaluation of aerosol mixing state classes in the GISS modelE - MATRIX climate model using single - particle mass spectrometry measurements, J. Geophys. Res-Atmos., 118, 9834-9844, 2013.

25 Brook, R. D., Franklin, B., Cascio, W., Hong, Y., Howard, G., Lipsett, M., Luepker, R., Mittleman, M., Samet, J., and Smith, S. C.: Air pollution and cardiovascular disease, Circulation, 109, 2655-2671, 2004.

Bullard, R. L., Singh, A., Anderson, S. M., Lehmann, C. M., and Stanier, C. O.: 10-Month characterization of the aerosol number size distribution and related air quality and meteorology at the Bondville, IL Midwestern background site, Atmos. Environ., 2017.

30 [Burling, I., Yokelson, R. J., Griffith, D. W., Johnson, T. J., Veres, P., Roberts, J., Warneke, C., Urbanski, S., Reardon, J., and Weise, D.: Laboratory measurements of trace gas emissions from biomass burning of fuel types from the southeastern and southwestern United States. Atmos. Chem. Phys., 10, 11115-11130, 2010.](#)

Calvo, A., Alves, C., Castro, A., Pont, V., Vicente, A., and Fraile, R.: Research on aerosol sources and 35 chemical composition: past, current and emerging issues, Atmospheric Research, 120, 1-28, 2013.

Canagaratna, M., Jimenez, J., Kroll, J., Chen, Q., Kessler, S., Massoli, P., Hildebrandt Ruiz, L., Fortner, E., Williams, L., and Wilson, K.: Elemental ratio measurements of organic compounds using aerosol mass spectrometry: characterization, improved calibration, and implications, 40 Atmos. Chem. Phys., 15, 253-272, 2015.

Carlton, A. G., Pinder, R. W., Bhave, P. V., and Pouliot, G. A.: To what extent can biogenic SOA be controlled?, *Environ. Sci. Technol.*, 44, 3376-3380, 2010.

Carroll, M. A., Bertman, S. B., and Shepson, P. B.: Overview of the Program for Research on Oxidants: Photochemistry, Emissions, and Transport (PROPHET) summer 1998 measurements intensive, *J. Geophys. Res.-Atmos.*, 106, 24275-24288, 2001.

Centre, C. I. F. F.:Canadian Interagency Forest Fire Centre, National Wildland Fire Situation Report: <http://www.cifrc.ca>, Accessed July 2016,

Colarco, P., Schoeberl, M., Doddridge, B., Marufu, L., Torres, O., and Welton, E.: Transport of smoke from Canadian forest fires to the surface near Washington, DC: Injection height, entrainment, and optical properties, *J. Geophys. Res.-Atmos.*, 109, D06203, 2004.

Cooper, O., Moody, J., Thornberry, T., Town, M., and Carroll, M.: PROPHET 1998 meteorological overview and air - mass classification, *J. Geophys. Res.-Atmos.*, 106, 24289-24299, 2001.

Creamean, J. M., Suski, K. J., Rosenfeld, D., Cazorla, A., DeMott, P. J., Sullivan, R. C., White, A. B., Ralph, F. M., Minnis, P., and Comstock, J. M.: Dust and biological aerosols from the Sahara and Asia influence precipitation in the western US, *Science*, 339, 1572-1578, 2013.

Dall'Osto, M., Beddows, D., Kinnersley, R. P., Harrison, R. M., Donovan, R. J., and Heal, M. R.: Characterization of individual airborne particles by using aerosol time - of - flight mass spectrometry at Mace Head, Ireland, *J. Geophys. Res.-Atmos.*, 109, 2004.

DeBell, L. J., Talbot, R. W., Dibb, J. E., Munger, J. W., Fischer, E. V., and Frolking, S. E.: A major regional air pollution event in the northeastern United States caused by extensive forest fires in Quebec, Canada, *J. Geophys. Res.-Atmos.*, 109, D19305, 2004.

DeCarlo, P. F., Kimmel, J. R., Trimborn, A., Northway, M. J., Jayne, J. T., Aiken, A. C., Gonin, M., Fuhrer, K., Horvath, T., and Docherty, K. S.: Field-deployable, high-resolution, time-of-flight aerosol mass spectrometer, *Anal. Chem.*, 78, 8281-8289, 2006.

Dempsey, F.: Forest fire effects on air quality in Ontario: Evaluation of several recent examples, *B. Am. Meteorol. Soc.*, 94, 1059-1064, 2013.

Dreessen, J., Sullivan, J., and Delgado, R.: Observations and Impacts of Transported Canadian Wildfire Smoke on Ozone and Aerosol Air Quality in the Maryland Region on 9-12 June, 2015, *J. Air Waste Manage. Assoc.*, 66, 842-862, 2016.

Dutkiewicz, V. A., Husain, L., Roychowdhury, U. K., and Demerjian, K. L.: Impact of Canadian wildfire smoke on air quality at two rural sites in NY State, *Atmos. Environ.*, 45, 2028-2033, 2011.

Emanuelsson, E. U., Hallquist, M., Kristensen, K., Glasius, M., Bohn, B., Fuchs, H., Kammer, B., Kiendler-Scharr, A., Nehr, S., and Rubach, F.: Formation of anthropogenic secondary organic aerosol (SOA) and its influence on biogenic SOA properties, *Atmos. Chem. Phys.*, 13, 2837-2855, 2013.

Farmer, D., Matsunaga, A., Docherty, K., Surratt, J., Seinfeld, J., Ziemann, P., and Jimenez, J.: Response of an aerosol mass spectrometer to organonitrates and organosulfates and implications for atmospheric chemistry, *Proc. Natl. Acad. Sci.*, 107, 6670-6675, 2010.

Fierce, L., Bond, T. C., Bauer, S. E., Mena, F., and Riemer, N.: Black carbon absorption at the global scale is affected by particle-scale diversity in composition, *Nat. Commun.*, 7, 2016.

Fitzgerald, E., Ault, A. P., Zauscher, M. D., Mayol-Bracero, O. L., and Prather, K. A.: Comparison of the mixing state of long-range transported Asian and African mineral dust, *Atmos. Environ.*, 115, 19-25, 2015.

Forster, C., Wandinger, U., Wotawa, G., James, P., Mattis, I., Althausen, D., Simmonds, P., O'Doherty, S., Jennings, S. G., and Kleefeld, C.: Transport of boreal forest fire emissions from Canada to Europe, *J. Geophys. Res.-Atmos.*, 106, 22887-22906, 2001.

Furutani, H., Dall'osto, M., Roberts, G. C., and Prather, K. A.: Assessment of the relative importance of atmospheric aging on CCN activity derived from field observations, *Atmos. Environ.*, 42, 3130-3142, 2008.

10 Gard, E., Mayer, J. E., Morrical, B. D., Dienes, T., Fergenson, D. P., and Prather, K. A.: Real-time analysis of individual atmospheric aerosol particles: Design and performance of a portable ATOFMS, *Anal. Chem.*, 69, 4083-4091, 1997.

Gillett, N., Weaver, A., Zwiers, F., and Flannigan, M.: Detecting the effect of climate change on Canadian forest fires, *Geophys. Res. Lett.*, 31, L18211, 2004.

15 Grieshop, A., Donahue, N., and Robinson, A.: Laboratory investigation of photochemical oxidation of organic aerosol from wood fires 2: analysis of aerosol mass spectrometer data, *Atmos. Chem. Phys.*, 9, 2227-2240, 2009.

Gunsch, M. J., Schmidt, S., Gardner, D. J., Bondy, A. L., May, N., Bertman, S. B., Pratt, K. A., and Ault, A. P.: Particle Growth in an Isoprene-Rich Forest: Influences of Urban, Wildfire, and Biogenic Precursors, Submitted/Accepted to *Atmospheric Environment*, 2017-2018.

20 Hennigan, C. J., Sullivan, A. P., Collett, J. L., and Robinson, A. L.: Levoglucosan stability in biomass burning particles exposed to hydroxyl radicals, *Geophys. Res. Lett.*, 37, 2010.

Hu, Y., Odman, M. T., Chang, M. E., Jackson, W., Lee, S., Edgerton, E. S., Baumann, K., and Russell, A. G.: Simulation of air quality impacts from prescribed fires on an urban area, *Environ. Sci. Technol.*, 42, 3676-3682, 2008.

25 Hudson, P. K., Murphy, D. M., Cziczo, D. J., Thomson, D. S., De Gouw, J. A., Warneke, C., Holloway, J., Jost, H. J., and Hübner, G.: Biomass - burning particle measurements: Characteristic composition and chemical processing, *J. Geophys. Res.-Atmos.*, 109, D23S27, 2004.

30 IPCC: IPCC, 2013: climate change 2013: the physical science basis. Contribution of working group I to the fifth assessment report of the intergovernmental panel on climate change, edited by: Stocker, T., Qin, D., Plattner, G., Tignor, M., Allen, S., Boschung, J., Nauels, A., Xia, Y., Bex, B., and Midgley, B., Cambridge University Press, 2013.

Jaffe, D. A., and Wigder, N. L.: Ozone production from wildfires: A critical review, *Atmos. Environ.*, 51, 1-10, 2012.

35 Jathar, S. H., Gordon, T. D., Hennigan, C. J., Pye, H. O., Pouliot, G., Adams, P. J., Donahue, N. M., and Robinson, A. L.: Unspeciated organic emissions from combustion sources and their influence on the secondary organic aerosol budget in the United States, *Proc. Natl. Acad. Sci.*, 111, 10473-10478, 2014.

Jayne, J. T., Leard, D. C., Zhang, X., Davidovits, P., Smith, K. A., Kolb, C. E., and Worsnop, D. R.: Development of an aerosol mass spectrometer for size and composition analysis of submicron particles, *Aerosol. Sci. Technol.*, 33, 49-70, 2000.

5 Jeong, C.-H., McGuire, M. L., Godri, K. J., Slowik, J. G., Rehbein, P., and Evans, G.: Quantification of aerosol chemical composition using continuous single particle measurements, *Atmos. Chem. Phys.*, 11, 7027-7044, 2011.

Jimenez, J., Canagaratna, M., Donahue, N., Prevot, A., Zhang, Q., Kroll, J. H., DeCarlo, P. F., Allan, J. D., Coe, H., and Ng, N.: Evolution of organic aerosols in the atmosphere, *Science*, 326, 1525-1529, 2009.

10 Jimenez, J., and DeCarlo, P.: Field ToF-AMS Operation: <http://www.ciffe.ca>, Accessed September 2017, http://cires1.colorado.edu/jimenez-group/wiki/index.php/Field_ToF-AMS_Operation, Accessed September 2017.

15 Jimenez, J. L., Jayne, J. T., Shi, Q., Kolb, C. E., Worsnop, D. R., Yourshaw, I., Seinfeld, J. H., Flagan, R. C., Zhang, X., and Smith, K. A.: Ambient aerosol sampling using the aerodyne aerosol mass spectrometer, *J. Geophys. Res.-Atmos.*, 108, 8425, 2003.

20 Kang, C.-M., Gold, D., and Koutrakis, P.: Downwind O₃ and PM 2.5 speciation during the wildfires in 2002 and 2010, *Atmos. Environ.*, 95, 511-519, 2014.

Khlystov, A., Stanier, C., and Pandis, S.: An algorithm for combining electrical mobility and aerodynamic size distributions data when measuring ambient aerosol, *Aerosol. Sci. Technol.*, 38, 229-238, 2004.

25 Kim, E., Hopke, P. K., Kenski, D. M., and Koerber, M.: Sources of fine particles in a rural midwestern US area, *Environ. Sci. Technol.*, 39, 4953-4960, 2005.

Kim, M., Deshpande, S. R., and Crist, K. C.: Source apportionment of fine particulate matter (PM2.5) at a rural Ohio River Valley site, *Atmos. Environ.*, 41, 9231-9243, 2007.

30 Knorr, W., Jiang, L., and Arneth, A.: Climate, CO₂ and human population impacts on global wildfire emissions, *Biogeosciences*, 13, 267-282, 2016.

Kundu, S., and Stone, E. A.: Composition and sources of fine particulate matter across urban and rural sites in the Midwestern United States, *Env. Sci. Process. Impact*, 16, 1360-1370, 2014.

35 Lee, A. K., Herckes, P., Leaitch, W., Macdonald, A., and Abbatt, J.: Aqueous OH oxidation of ambient organic aerosol and cloud water organics: Formation of highly oxidized products, *Geophys. Res. Lett.*, 38, 2011.

Liu, X., Zhang, Y., Huey, L., Yokelson, R., Wang, Y., Jimenez, J., Campuzano - Jost, P., Beyersdorf, A., Blake, D., and Choi, Y.: Agricultural fires in the southeastern US during SEAC4RS: Emissions of trace gases and particles and evolution of ozone, reactive nitrogen, and organic aerosol, *J. Geophys. Res.-Atmos.*, 121, 7383-7414, 2016.

40 Liu, Y., Stanturf, J., and Goodrick, S.: Trends in global wildfire potential in a changing climate, *Forest. Ecol. Manag.*, 259, 685-697, 2010.

Lu, X., Zhang, L., Yue, X., Zhang, J., Jaffe, D. A., Stohl, A., Zhao, Y., and Shao, J.: Wildfire influences on the variability and trend of summer surface ozone in the mountainous western United States, *Atmos. Chem. Phys.*, 16, 14687-14702, 2016.

Matsui, H., Koike, M., Kondo, Y., Moteki, N., Fast, J. D., and Zaveri, R. A.: Development and validation of a black carbon mixing state resolved three - dimensional model: Aging processes and radiative impact, *J. Geophys. Res-Atmos.*, 118, 2304-2326, 2013.

5 [May, N. W., Olson, N. E., Panas, M., Axson, J. L., Tirella, P. S., Kirpes, R. M., Craig, R. L., Gunsch, M. J., China, S., Laskin, A., Ault, A. P., and Pratt, K. A.: Aerosol Emissions from Great Lakes Harmful Algal Blooms. Environ. Sci. Technol.](#), 52, 397-405, 10.1021/acs.est.7b03609, 2018.

Middlebrook, A. M., Bahreini, R., Jimenez, J. L., and Canagaratna, M. R.: Evaluation of composition-dependent collection efficiencies for the aerodyne aerosol mass spectrometer using field data, *Aerosol. Sci. Technol.*, 46, 258-271, 2012.

10 Miller, D. J., Sun, K., Zondlo, M. A., Kanter, D., Dubovik, O., Welton, E. J., Winker, D. M., and Ginoux, P.: Assessing boreal forest fire smoke aerosol impacts on US air quality: A case study using multiple data sets, *J. Geophys. Res-Atmos.*, 116, 2011.

Moffet, R. C., Qin, X., Rebotier, T., Furutani, H., and Prather, K. A.: Chemically segregated optical and microphysical properties of ambient aerosols measured in a single - particle mass spectrometer, *J. Geophys. Res-Atmos.*, 113, D12213, 2008.

15 Moffet, R. C., and Prather, K. A.: In-situ measurements of the mixing state and optical properties of soot with implications for radiative forcing estimates, *Proc. Natl. Acad. Sci.*, 106, 11872-11877, 2009.

Moffet, R. C., Henn, T. R., Tivanski, A. V., Hopkins, R. J., Desyaterik, Y., Kilcoyne, A., Tyliszczak, T., Fast, J., Barnard, J., and Shutthanandan, V.: Microscopic characterization of carbonaceous aerosol particle aging in the outflow from Mexico City, *Atmos. Chem. Phys.*, 10, 961-976, 2010.

20 Müller, D., Mattis, I., Wandinger, U., Ansmann, A., Althausen, D., and Stohl, A.: Raman lidar observations of aged Siberian and Canadian forest fire smoke in the free troposphere over Germany in 2003: Microphysical particle characterization, *J. Geophys. Res-Atmos.*, 110, 2005.

25 National Research Council, and National Academies: Global sources of local pollution: an assessment of long-range transport of key air pollutants to and from the United States, xiii, 234 p., National Academies Press, Washington, D.C., xiii, 234 p. pp., 2010.

Pastor, S. H., Allen, J. O., Hughes, L. S., Bhave, P., Cass, G. R., and Prather, K. A.: Ambient single particle analysis in Riverside, California by aerosol time-of-flight mass spectrometry during the SCOS97-NARSTO, *Atmos. Environ.*, 37, 239-258, 2003.

30 Paulot, F., Jacob, D. J., Pinder, R., Bash, J., Travis, K., and Henze, D.: Ammonia emissions in the United States, European Union, and China derived by high - resolution inversion of ammonium wet deposition data: Interpretation with a new agricultural emissions inventory (MASAGE_NH3), *J. Geophys. Res-Atmos.*, 119, 4343-4364, 2014.

35 Petters, M. D., Carrico, C. M., Kreidenweis, S. M., Prenni, A. J., DeMott, P. J., Collett, J. L., and Moosmueller, H.: Cloud condensation nucleation activity of biomass burning aerosol, *J. Geophys. Res-Atmos.*, 114, 2009.

Pope, C. A., and Dockery, D. W.: Health effects of fine particulate air pollution: lines that connect, *J. Air Waste Manage. Assoc.*, 56, 709-742, 2006.

Pöschl, U.: Atmospheric Aerosols: Composition, Transformation, Climate and Health Effects, *Angew. Chem. Int. Ed.*, 44, 7520 - 7540, 2005.

Pöschl, U., and Shiraiwa, M.: Multiphase chemistry at the atmosphere-biosphere interface influencing climate and public health in the anthropocene, *Chem. Rev.*, 115, 4440-4475, 2015.

Pratt, K., Murphy, S., Subramanian, R., DeMott, P., Kok, G., Campos, T., Rogers, D., Prenni, A., Heymsfield, A., and Seinfeld, J.: Flight-based chemical characterization of biomass burning aerosols within two prescribed burn smoke plumes, *Atmos. Chem. Phys.*, 11, 12549-12565, 2011.

Pratt, K. A., and Prather, K. A.: Real-time, single-particle volatility, size, and chemical composition measurements of aged urban aerosols, *Environ. Sci. Technol.*, 43, 8276-8282, 2009.

Pratt, K. A., Heymsfield, A. J., Twohy, C. H., Murphy, S. M., DeMott, P. J., Hudson, J. G., Subramanian, R., Wang, Z., Seinfeld, J. H., and Prather, K. A.: In situ chemical characterization of aged biomass-burning aerosols impacting cold wave clouds, *J. Atmos. Sci.*, 67, 2451-2468, 2010.

Pratt, K. A., and Prather, K. A.: Mass spectrometry of atmospheric aerosols—Recent developments and applications. Part II: On - line mass spectrometry techniques, *Mass Spectrom. Rev.*, 31, 17-48, 2012.

Qin, X., Bhave, P. V., and Prather, K. A.: Comparison of two methods for obtaining quantitative mass concentrations from aerosol time-of-flight mass spectrometry measurements, *Anal. Chem.*, 78, 6169-6178, 2006.

Qin, X., Pratt, K. A., Shields, L. G., Toner, S. M., and Prather, K. A.: Seasonal comparisons of single-particle chemical mixing state in Riverside, CA, *Atmos. Environ.*, 59, 587-596, 2012.

Raatikainen, T., Vaattovaara, P., Tiitta, P., Miettinen, P., Rautiainen, J., Ehn, M., Kulmala, M., Laaksonen, A., and Worsnop, D. R.: Physicochemical properties and origin of organic groups detected in boreal forest using an aerosol mass spectrometer, *Atmos. Chem. Phys.*, 10, 2063-2077, 2010.

Rattanavaraha, W., Chu, K., Budisulistiorini, S. H., Riva, M., Lin, Y.-H., Edgerton, E. S., Baumann, K., Shaw, S. L., Guo, H., and King, L.: Assessing the impact of anthropogenic pollution on isoprene-derived secondary organic aerosol formation in PM 2.5 collected from the Birmingham, Alabama, ground site during the 2013 Southern Oxidant and Aerosol Study, *Atmos. Chem. Phys.*, 16, 4897-4914, 2016.

Riemer, N., and West, M.: Quantifying aerosol mixing state with entropy and diversity measures, *Atmos. Chem. Phys.*, 13, 11423-11439, 2013.

Rolph, G. D., Draxler, R. R., Stein, A. F., Taylor, A., Ruminski, M. G., Kondragunta, S., Zeng, J., Huang, H.-C., Manikin, G., and McQueen, J. T.: Description and verification of the NOAA smoke forecasting system: the 2007 fire season, *Weather Forecast.*, 24, 361-378, 2009.

[Seinfeld, J. H., and Pandis, S. N.: Atmospheric chemistry and physics: from air pollution to climate change. John Wiley & Sons, Hoboken, New Jersey, 2016.](#)

Sheesley, R. J., Schauer, J. J., Bean, E., and Kenski, D.: Trends in secondary organic aerosol at a remote site in Michigan's upper peninsula, *Environ. Sci. Technol.*, 38, 6491-6500, 2004.

Silva, P. J., Liu, D.-Y., Noble, C. A., and Prather, K. A.: Size and chemical characterization of individual particles resulting from biomass burning of local Southern California species, *Environ. Sci. Technol.*, 33, 3068-3076, 1999.

5 Sjostedt, S., Slowik, J., Brook, J., Chang, R.-W., Mihele, C., Stroud, C., Vlasenko, A., and Abbatt, J.: Diurnally resolved particulate and VOC measurements at a rural site: indication of significant biogenic secondary organic aerosol formation, *Atmos. Chem. Phys.*, 11, 5745-5760, 2011.

10 Slowik, J., Stroud, C., Bottenheim, J., Brickell, P., Chang, R.-W., Liggio, J., Makar, P., Martin, R., Moran, M., and Shantz, N.: Characterization of a large biogenic secondary organic aerosol event from eastern Canadian forests, *Atmos. Chem. Phys.*, 10, 2825-2845, 2010.

15 Slowik, J., Brook, J., Chang, R.-W., Evans, G., Hayden, K., Jeong, C.-H., Li, S.-M., Liggio, J., Liu, P., and McGuire, M.: Photochemical processing of organic aerosol at nearby continental sites: contrast between urban plumes and regional aerosol, *Atmos. Chem. Phys.*, 11, 2991-3006, 2011.

20 Smith, S., and Mueller, S.: Modeling natural emissions in the Community Multiscale Air Quality (CMAQ) Model-I: building an emissions data base, *Atmos. Chem. Phys.*, 10, 4931-4952, 2010.

Song, X.-H., Hopke, P. K., Fergenson, D. P., and Prather, K. A.: Classification of single particles analyzed by ATOFMS using an artificial neural network, ART-2A, *Anal. Chem.*, 71, 860-865, 1999.

25 Spencer, M. T., Shields, L. G., and Prather, K. A.: Simultaneous measurement of the effective density and chemical composition of ambient aerosol particles, *Environ. Sci. Technol.*, 41, 1303-1309, 2007.

Stephen, K., and Aneja, V. P.: Trends in agricultural ammonia emissions and ammonium concentrations in precipitation over the Southeast and Midwest United States, *Atmos. Environ.*, 42, 3238-3252, 2008.

30 Stockwell, C., Yokelson, R., Kreidenweis, S., Robinson, A., DeMott, P., Sullivan, R., Reardon, J., Ryan, K., Griffith, D., and Stevens, L.: Trace gas emissions from combustion of peat, crop residue, domestic biofuels, grasses, and other fuels: configuration and Fourier transform infrared (FTIR) component of the fourth Fire Lab at Missoula Experiment (FLAME-4), *Atmos. Chem. Phys.*, 9727, 2014.

35 Su, Y., Sipin, M. F., Furutani, H., and Prather, K. A.: Development and characterization of an aerosol time-of-flight mass spectrometer with increased detection efficiency, *Anal. Chem.*, 76, 712-719, 2004.

Sueper, D.: ToF-AMS analysis software, Available at: <http://cires1.colorado.edu/jimenez-group/ToFAMSResources/ToFSoftware/index.html>, 2010.

35 Sullivan, R., Guazzotti, S., Sodeman, D., and Prather, K.: Direct observations of the atmospheric processing of Asian mineral dust, *Atmos. Chem. Phys.*, 7, 1213-1236, 2007.

40 Sun, Y., Zhang, Q., Macdonald, A. M., Hayden, K., Li, S. M., Liggio, J., Liu, P. S. K., Anlauf, K. G., Leaitch, W. R., Steffen, A., Cubison, M., Worsnop, D. R., van Donkelaar, A., and Martin, R. V.: Size-resolved aerosol chemistry on Whistler Mountain, Canada with a high-resolution aerosol

mass spectrometer during INTEX-B, *Atmos. Chem. Phys.*, 9, 3095-3111, 10.5194/acp-9-3095-2009, 2009.

5 Toner, S. M., Sodeman, D. A., and Prather, K. A.: Single particle characterization of ultrafine and accumulation mode particles from heavy duty diesel vehicles using aerosol time-of-flight mass spectrometry, *Environ. Sci. Technol.*, 40, 3912-3921, 2006.

Toner, S. M., Shields, L. G., Sodeman, D. A., and Prather, K. A.: Using mass spectral source signatures to apportion exhaust particles from gasoline and diesel powered vehicles in a freeway study using UF-ATOFMS, *Atmos. Environ.*, 42, 568-581, 2008.

10 Uno, I., Eguchi, K., Yumimoto, K., Takemura, T., Shimizu, A., Uematsu, M., Liu, Z., Wang, Z., Hara, Y., and Sugimoto, N.: Asian dust transported one full circuit around the globe, *Nat. Geosci.*, 2, 557-560, 2009.

15 VanReken, T., Mwaniki, G., Wallace, H., Pressley, S., Erickson, M., Jobson, B., and Lamb, B.: Influence of air mass origin on aerosol properties at a remote Michigan forest site, *Atmos. Environ.*, 107, 35-43, 2015.

15 Veira, A., Lasslop, G., and Kloster, S.: Wildfires in a warmer climate: Emission fluxes, emission heights, and black carbon concentrations in 2090–2099, *J. Geophys. Res-Atmos.*, 121, 3195-3223, 2016.

20 Wang, J., Cubison, M., Aiken, A., Jimenez, J., and Collins, D.: The importance of aerosol mixing state and size-resolved composition on CCN concentration and the variation of the importance with atmospheric aging of aerosols, *Atmos. Chem. Phys.*, 10, 7267-7283, 2010a.

25 Wang, Y., Huang, J., Zananski, T. J., Hopke, P. K., and Holsen, T. M.: Impacts of the Canadian forest fires on atmospheric mercury and carbonaceous particles in northern New York, *Environ. Sci. Technol.*, 44, 8435-8440, 2010b.

30 Wiedinmyer, C., Quayle, B., Geron, C., Belote, A., McKenzie, D., Zhang, X., O'Neill, S., and Wynne, K. K.: Estimating emissions from fires in North America for air quality modeling, *Atmos. Environ.*, 40, 3419-3432, 2006.

35 Xu, L., Guo, H., Boyd, C. M., Klein, M., Bougiatioti, A., Cerully, K. M., Hite, J. R., Isaacman-VanWertz, G., Kreisberg, N. M., and Knote, C.: Effects of anthropogenic emissions on aerosol formation from isoprene and monoterpenes in the southeastern United States, *Proc. Natl. Acad. Sci.*, 112, 37-42, 2015.

Zhang, Y., Sheesley, R. J., Schauer, J. J., Lewandowski, M., Jaoui, M., Offenberg, J. H., Kleindienst, T. E., and Edney, E. O.: Source apportionment of primary and secondary organic aerosols using positive matrix factorization (PMF) of molecular markers, *Atmos. Environ.*, 43, 5567-5574, 2009.

35 Zhou, S., Collier, S., Jaffe, D. A., Briggs, N. L., Hee, J., Sedlacek III, A. J., Kleinman, L., Onasch, T. B., and Zhang, Q.: Regional influence of wildfires on aerosol chemistry in the western US and insights into atmospheric aging of biomass burning organic aerosol, *Atmos. Chem. Phys.*, 17, 2477-2493, 2017.

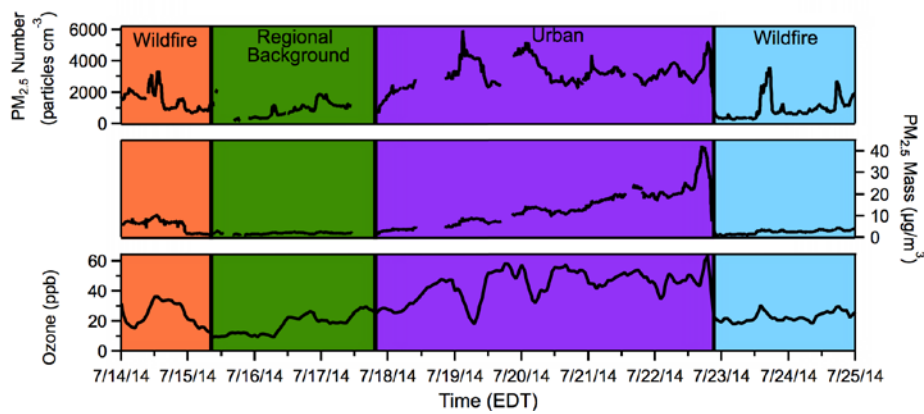


Figure 1. Time-resolved PM_{2.5} number and mass concentrations and ozone mole ratios during the different periods of air mass influence. Periods without data are due to instrument down time. Colors of the different time periods correspond to the colors of the corresponding HYSPLIT backward air mass

5

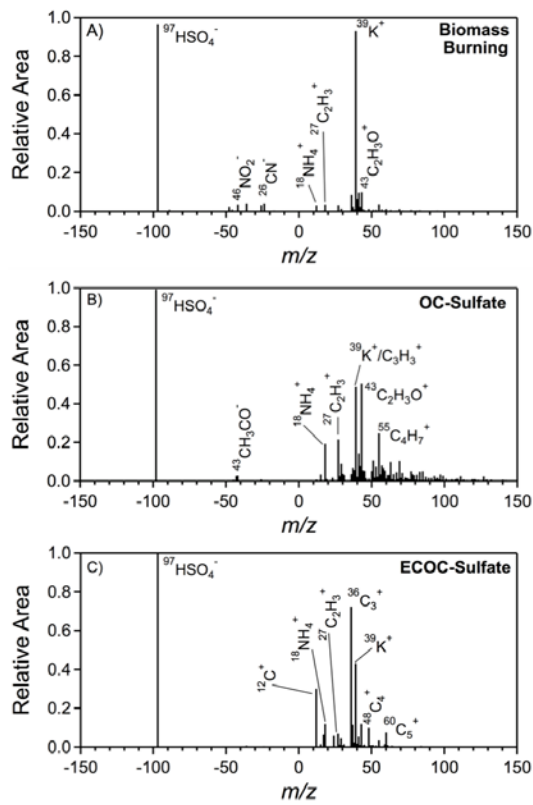


Figure 2. Average positive and negative ion single-particle mass spectra (ATOFMS), with characteristic peaks labeled, for the dominant aged combustion particle types observed: (A) biomass burning, (B) OC-Sulfate, and (C) ECOC-Sulfate.

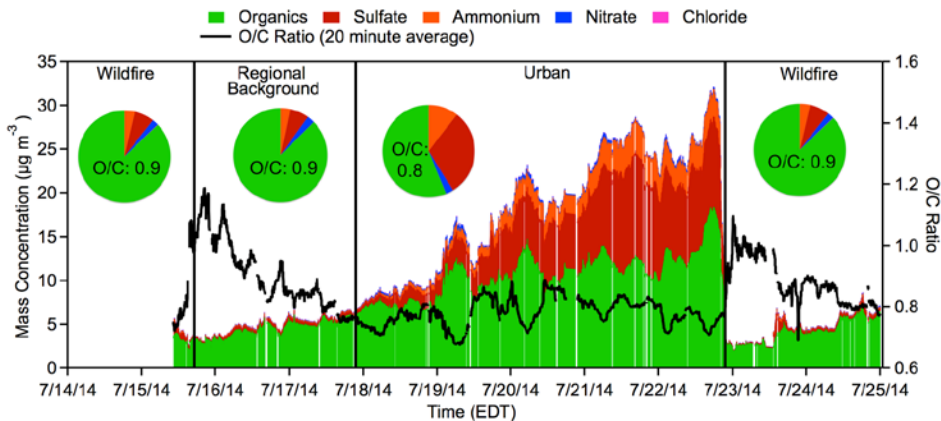


Figure 3. PM₁ non-refractory chemically speciated mass concentrations, as well as O/C ratios (20 min averages), measured by HR-AMS. Periods of influence are notated and separated by solid vertical lines. Pie charts represent the average mass fractions for each air mass period, with average O/C ratio inset.

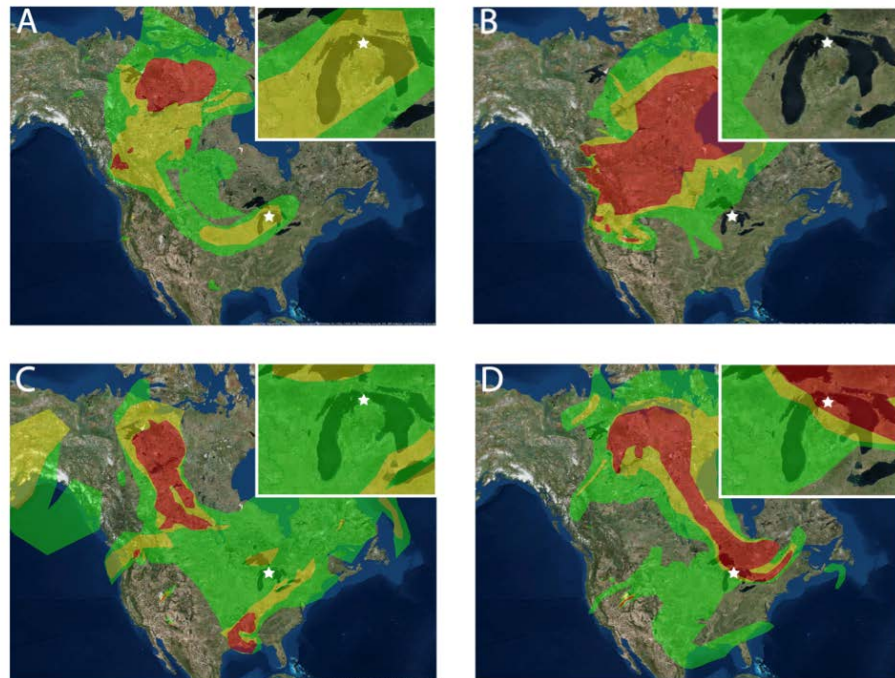


Figure 4. Representative NOAA HMS smoke maps for four representative days during the time periods of different air influence: (A) July 14, wildfire influence; (B) July 16, remote background influence; (C) July 21, Urban influence; (D) July 24, wildfire influence. Inset enlarges the state of Michigan to clearly

5 display smoke influence on the field site, shown as a star.

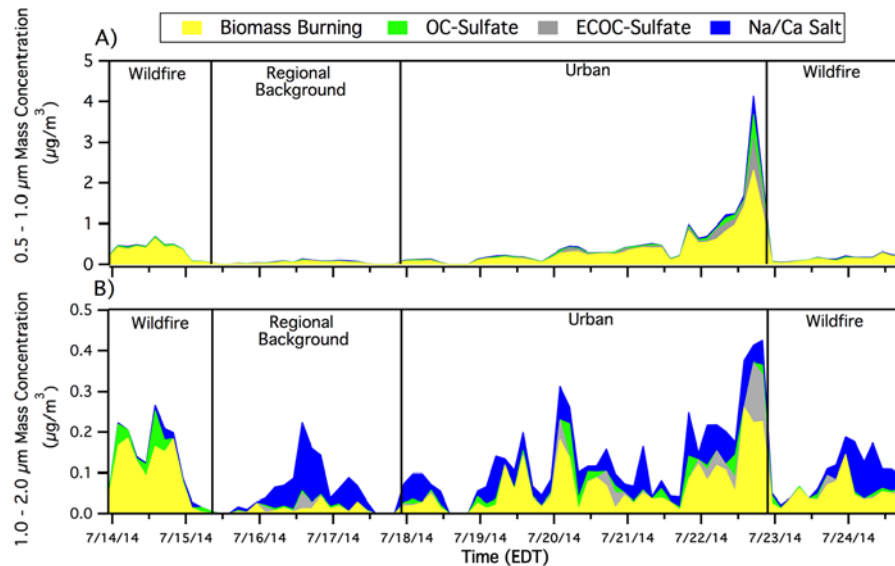
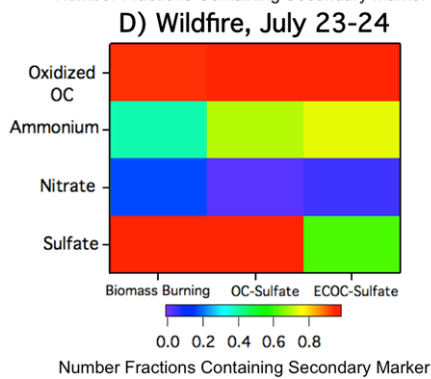
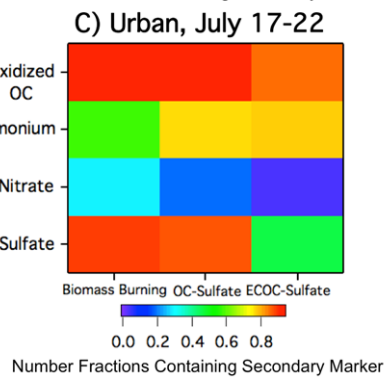
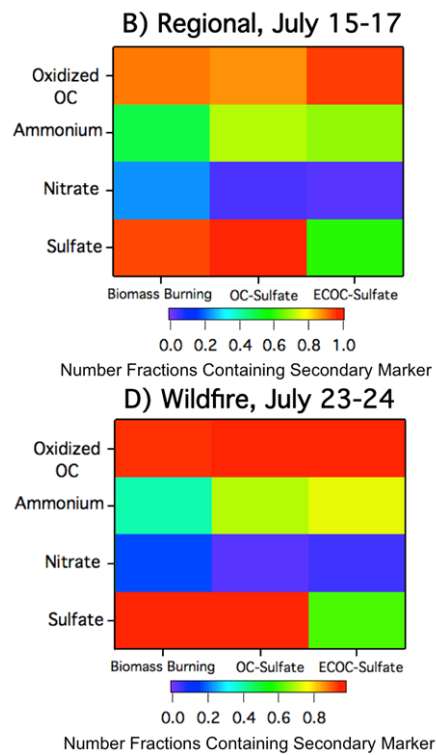
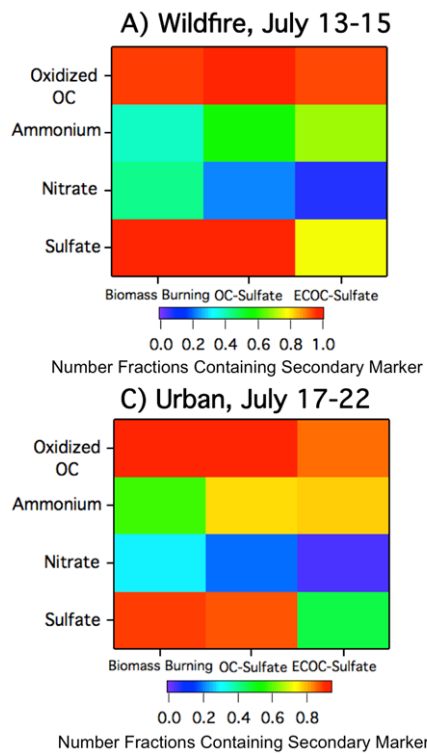


Figure 5. Three hour binned mass concentrations of (A) $0.5 - 1.0 \mu\text{m}$ and (B) $1.0 - 2.0 \mu\text{m}$ particle types, as measured by ATOFMS. Gaps in the data correspond to periods when APS data were not available for scaling.

5



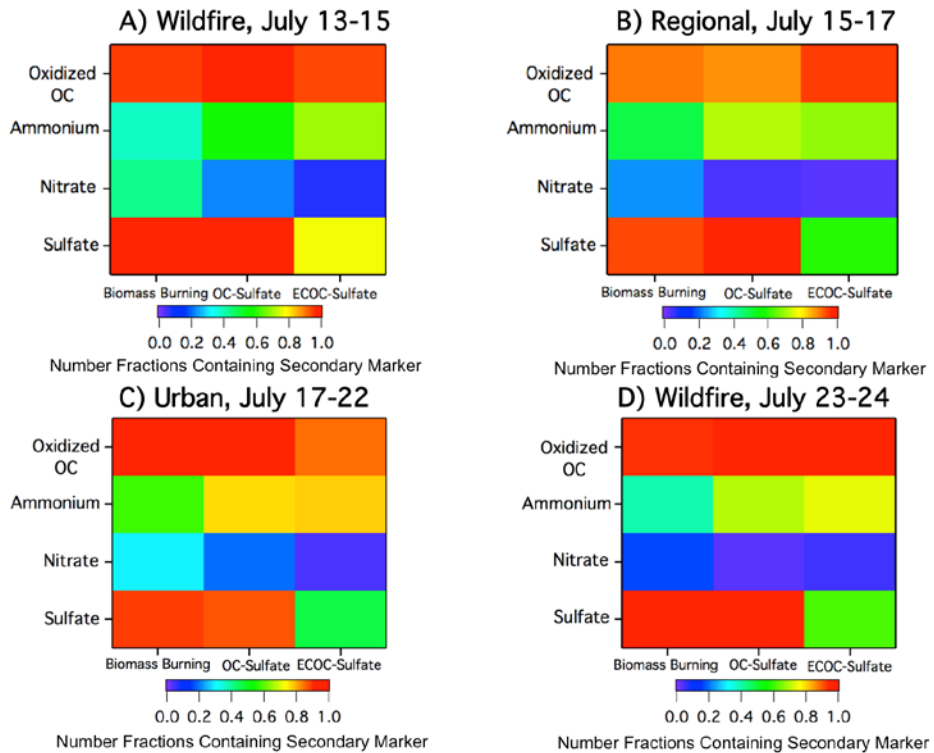


Figure 6. Number fractions of individual biomass burning, OC-sulfate, and ECOC-sulfate particles that were internally mixed with secondary species, as determined by ATOFMS ion markers, including oxidized OC ($C_2H_3O^+$, m/z 43), ammonium (NH_4^+ , m/z 18), nitrate (NO_2^- , m/z -46, and/or NO_3^- , m/z -62), and sulfate (HSO_4^- , m/z -97). Since a given particle can contain more than one secondary species, the number fractions can add to greater than one for a given particle type. Chemical mixing states are provided here for the four air mass time periods: (A) wildfire influence from July 13-15, (B) clean air from northern Canada from July 15-17, (C) mix of wildfire and urban influences from July 17-22, (D) mix of clean air and Canadian wildfires from July 23-24.

Supplemental Information for Ubiquitous Influence of Wildfire Emissions and Secondary Organic Aerosol on Summertime Atmospheric Aerosol in the Forested Great Lakes Region

5 Matthew J. Gunsch¹, Nathaniel W. May¹, Miao Wen², Courtney L. H. Bottemus^{2,3}, Daniel J. Gardner¹, Timothy M. VanReken^{2,†}, Steven B. Bertman⁴, Philip K. Hopke^{5,6}, Andrew P. Ault^{1,7}, Kerri A. Pratt^{1,8}

¹Department of Chemistry, University of Michigan, Ann Arbor, MI

²Department of Civil and Environmental Engineering, Washington State University, Pullman, WA

³Pacific Northwest National Laboratory, Richland, WA

10 ⁴Department of Chemistry, Western Michigan University, Kalamazoo, MI

⁵Center for Air Resources, Engineering and Science, Clarkson University, Potsdam, NY

⁶Department of Public Health Sciences, University of Rochester School of Medicine and Dentistry, Rochester, NY

⁷Department of Environmental Health Sciences, University of Michigan, Ann Arbor, MI

15 ⁸Department of Earth and Environmental Science, University of Michigan, Ann Arbor, MI

†Now at the National Science Foundation, Arlington, VA

Correspondence to: Kerri A. Pratt (prattka@umich.edu), Andrew P. Ault (aulta@umich.edu)

1 Supporting Measurements

Meteorological data (Figure S1), including wind direction, wind speed, relative humidity, and temperature, were collected by a Vaisala WXT510 weather sensor located at the top of the PROPHET tower. Variations in meteorological conditions throughout the study, and average meteorological conditions during each period of influence, are discussed in the main text. In order to determine the origin of the influential air masses (Figure S2), backward air mass trajectories were calculated using the NOAA Hybrid Single Particle Lagrangian Integrated Trajectory (HYSPLIT) Model (Stein et al., 2015). A final altitude of 500 m AGL was used for the field site, with each trajectory modeling the proceeding 72 h. During each of the three influence air mass locations, median, as well as 25th and 75th percentile aerosol number, mass, and size distributions were calculated based on SMPS measurements (Figures S3 and S4). Predicted NH₄⁺ (Figure S4) was calculated using the methods described by Sueper (2010). Though these calculations indicate the aerosol is likely acidic, there are caveats associated with these calculations, as outlined by Hennigan et al. (2015). Therefore, the pH cannot be reliably calculated beyond a qualitative indication of whether or not the aerosol is acidic.

References

Hennigan, C.J., Izumi, J., Sullivan, A.P., Weber, R.J., Nenes, A., 2015. A critical evaluation of proxy methods used to estimate the acidity of atmospheric particles. *Atmos. Chem. Phys.* 15, 2775-2790.

Stein, A., Draxler, R., Rolph, G., Stunder, B., Cohen, M., Ngan, F., 2015. NOAA's HYSPLIT atmospheric transport and dispersion modeling system. *B. Am. Meteorol. Soc.* 96, 2059-2077.

Sueper, D., 2010. ToF-AMS analysis software. Available at: <http://cires1.colorado.edu/jimenez-group/ToFAMSResources/ToFSoftware/index.html>.

VanReken, T., Mwaniki, G., Wallace, H., Pressley, S., Erickson, M., Jobson, B., and Lamb, B.: Influence of air mass origin on aerosol properties at a remote Michigan forest site, *Atmos. Environ.*, 107, 35-43, 2015.

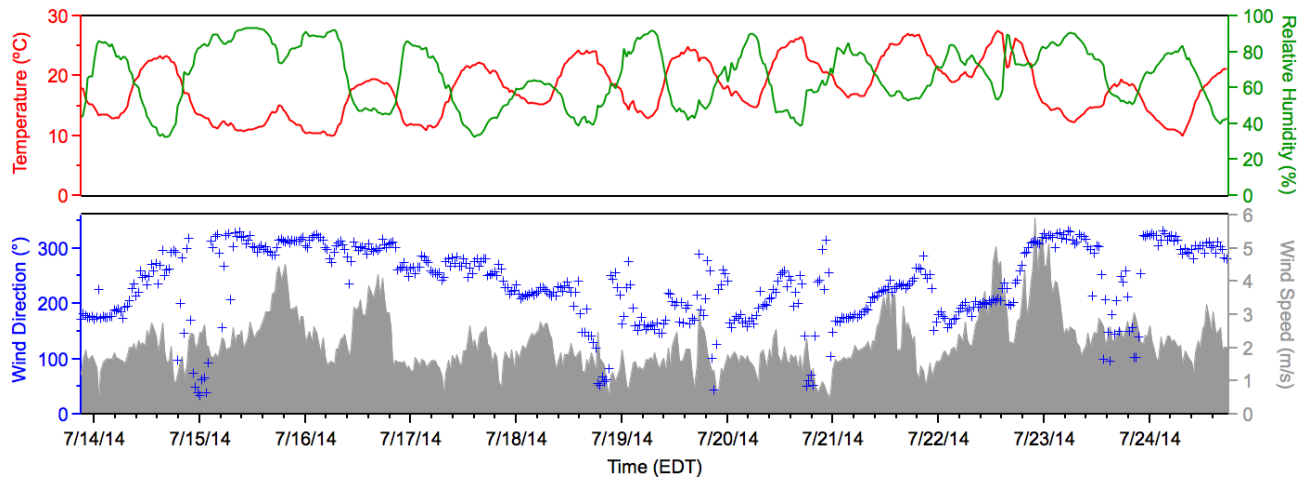


Figure S1. Meteorological conditions measured from a height of ~30 m at the UMBS PROPHET Tower.

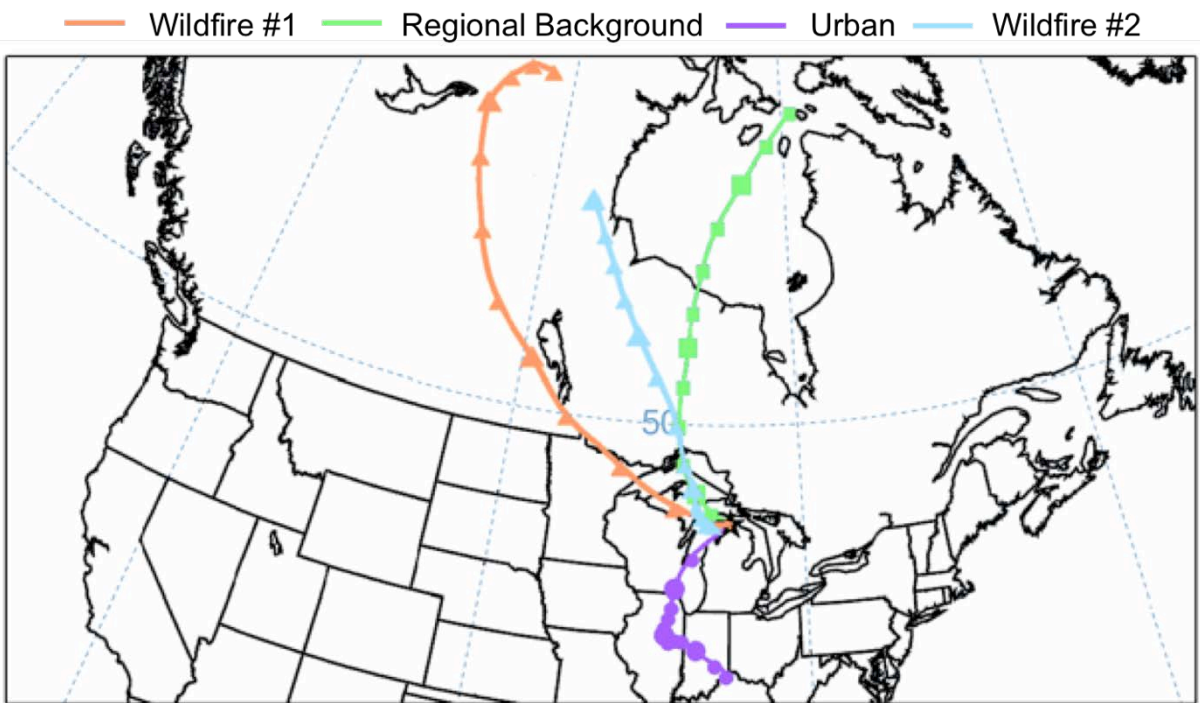
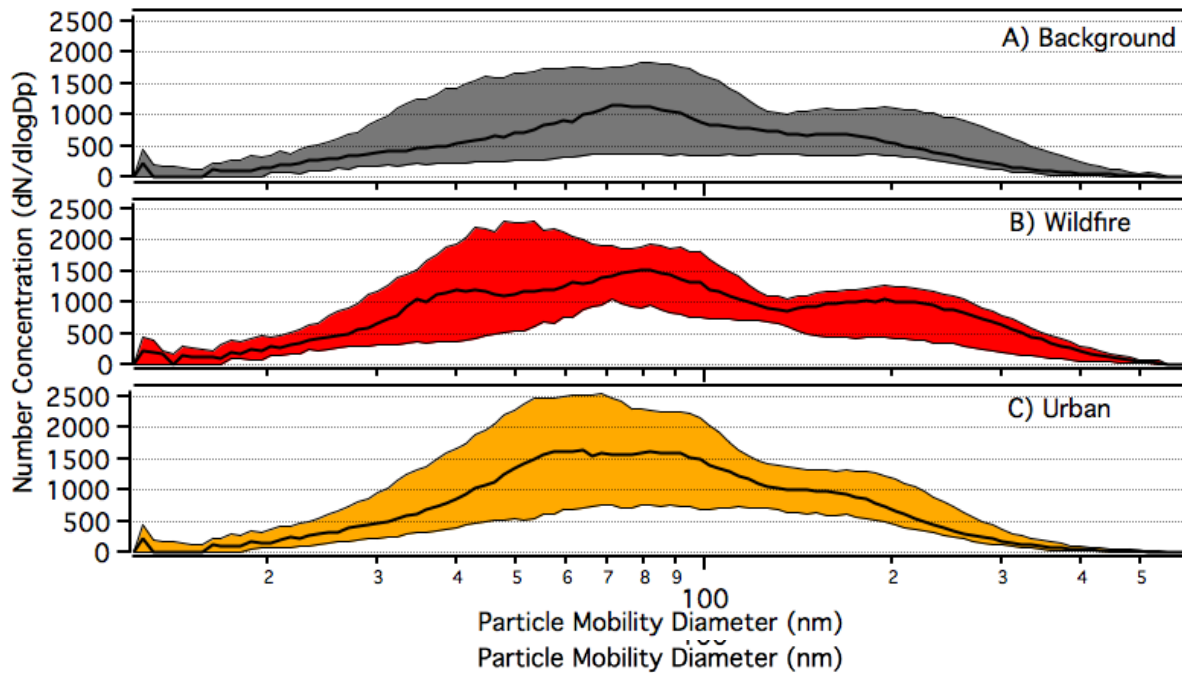


Figure S2. Representative 72 h HYSPLIT back trajectories with a final altitude of 500 m for the four air mass influences, with markers indicating 6 h intervals. Trajectory start times were: Wildfire #1: 7/14/2014 07:00 EDT, Regional Background: 7/17/2014 07:00 EDT, Urban: 7/21/2014 07:00 EDT, Wildfire #2: 7/24/14 07:00 EDT. Colors correspond to the air mass of influence indicated in Figure 3.



20

Figure S3. Median and 25th/75th percentiles of size-resolved particle number concentration distributions, as measured by SMPS, during the three air mass periods of interest: (A) Background, (B) Wildfire, and (C) Urban. For comparison, particle size distributions by air mass origin at UMBS in summer 2009 were previously discussed in detail by VanReken et al. (2015).

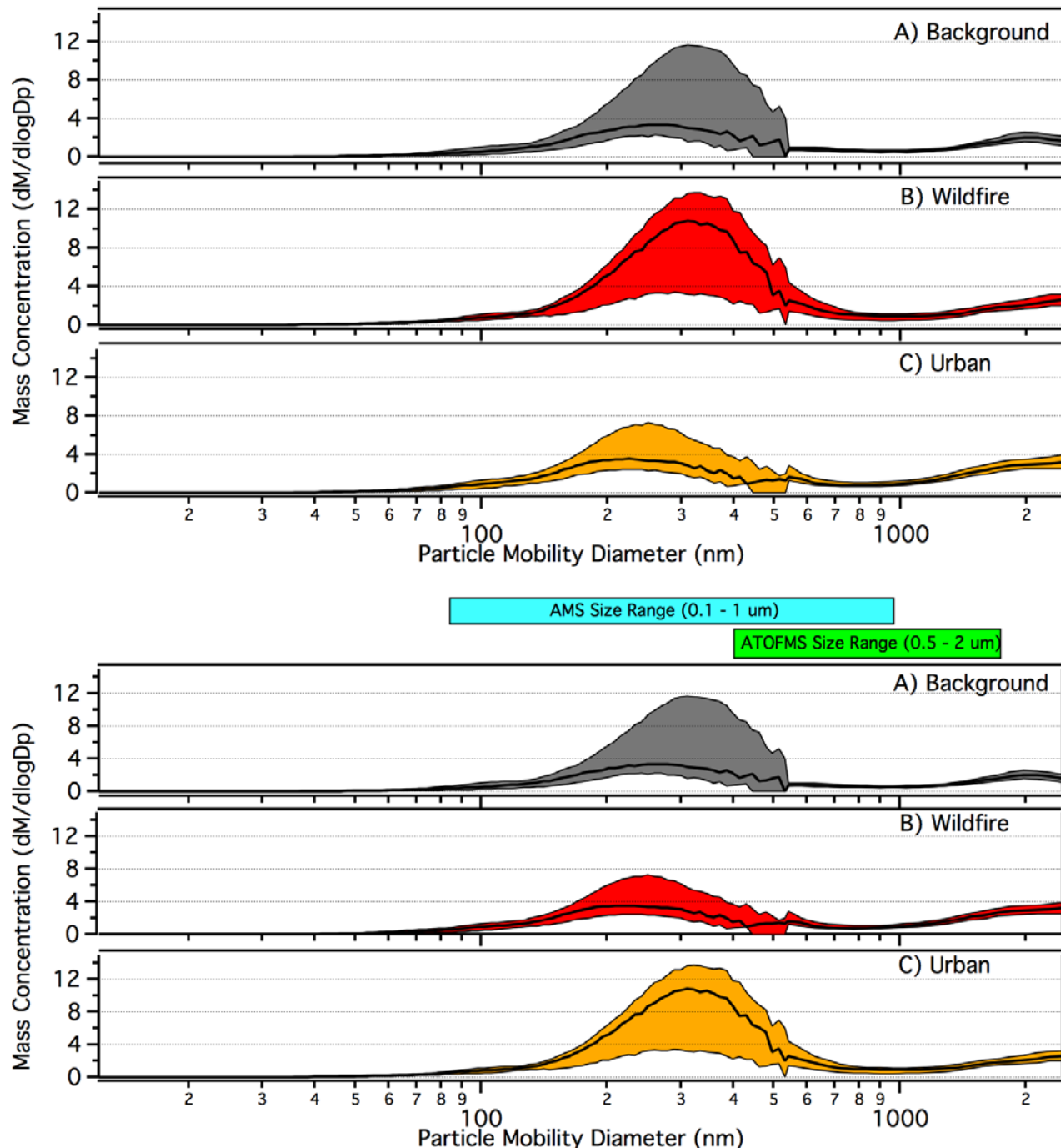


Figure S4. Median and 25th/75th percentiles of size-resolved particle mass distributions, as measured by SMPS and APS (assuming a density of 1.5 g cm^{-3}), during the three air mass periods of interest: (A) Background, (B) Wildfire, and (C) Urban. For comparison, the size range of measurements (converted

from vacuum aerodynamic diameter to mobility diameter) made by the AMS (blue) and ATOFMS (green) throughout the study are notated above the figure.

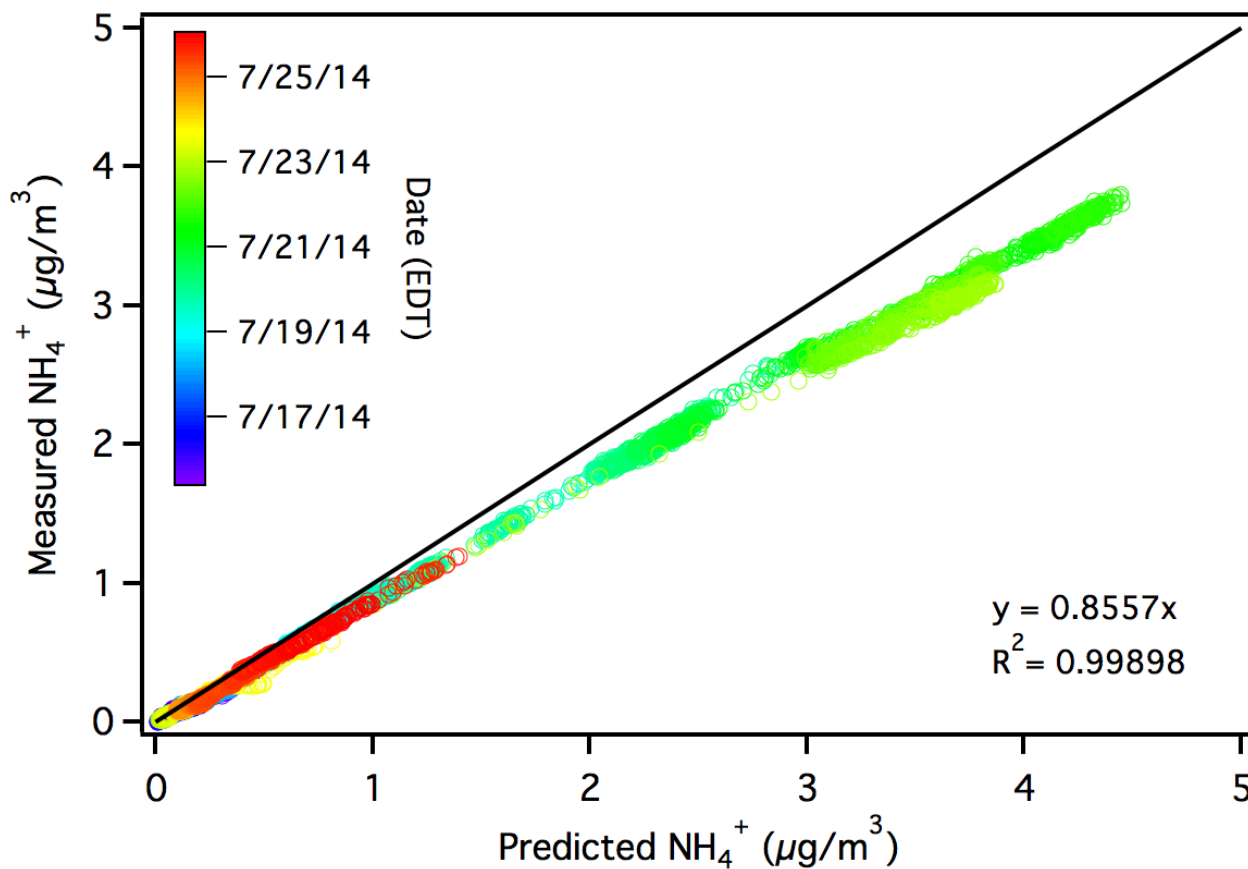


Figure S5. Ammonium balance calculated from predicted ammonium versus measured ammonium from the HR-AMS, following the method of Sueper (2010). A 1:1 line is showed in black for reference.

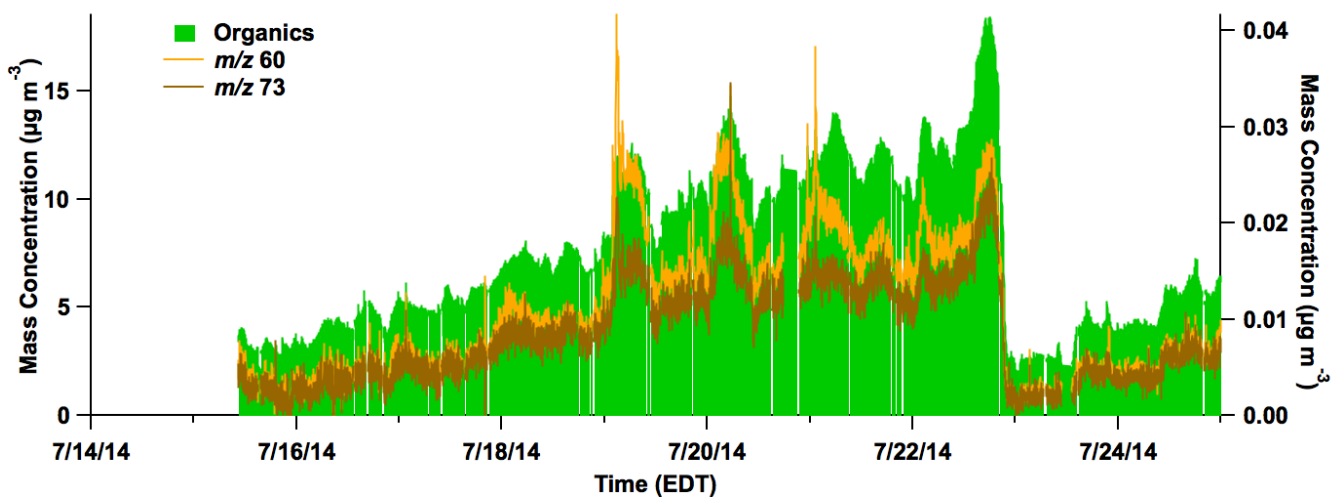


Figure S6. PM₁ non-refractory organic mass concentrations measured by HR-AMS (Figure 3), as well as specific tracers associated with biomass burning (m/z 60, $\text{C}_2\text{H}_4\text{O}_2^+$, and m/z 73, $\text{C}_3\text{H}_5\text{O}_2^+$) for comparison.